HHS Public Access

Author manuscript

Transl Res. Author manuscript; available in PMC 2024 July 01.

Published in final edited form as:

Transl Res. 2023 July ; 257: 1–14. doi:10.1016/j.trsl.2023.01.004.

AAV-based gene therapy prevents and halts the progression of dilated cardiomyopathy in a mouse model of phosphoglucomutase I deficiency (PGM1-CDG)

B Balakrishnan[1,^], **R Altassan**[2,^], **R Budhraja**[3], **W Liou**[4], **A Lupo**[1], **S Bryant**[1], **A Mankouski**[5], **S Radenkovic**[6], **G Preston**[6], **A Pandey**[3,7], **S Boudina**[8], **T Kozicz**[3,6,9,*], **E Morava**[3,6,10,*], **K Lai**[1,8,*]

[1]Division of Medical Genetics, Department of Pediatrics, University of Utah, Salt Lake City, USA

[2]Department of Medical Genomics, Centre for Genomic Medicine, King Faisal Specialist Hospital and Research Center, Riyadh, Saudi Arabia

[3]Department of Laboratory Medicine and Pathology, Mayo Clinic, Rochester, MN 55905, USA

[4]Electron Microscopy Core Facility, University of Utah, Salt Lake City, USA

[5]Division of Neonatology, Department of Pediatrics, University of Utah, Salt Lake City, USA

[6]Department of Clinical Genomics, Center of Individualized Medicine, Mayo Clinic, Rochester, USA

[7]Manipal Academy of Higher Education (MAHE), Manipal 576104, Karnataka, India

[8]Department of Nutrition and Integrative Physiology, College of Health, University of Utah, Salt Lake City, USA

[9]Department of Anatomy, University of Pecs School of Medicine, Pecs, Hungary

[10]Department of Medical Genetics, University of Pecs, School of Medicine, Pecs, Hungary

Abstract

PGM1 deficiency is recognized as the third most common *N*-linked Congenital Disorders of Glycosylation (CDG) in humans. Affected individuals present with liver, musculoskeletal, endocrine, and coagulation symptoms; however, the most life-threatening complication is the early onset of dilated cardiomyopathy (DCM). Recently, we discovered that oral D-galactose supplementation improved liver disease, endocrine and coagulation abnormalities, but does not

[*]Correspondence: Kent Lai, Ph.D. Division of Medical Genetics, Department of Pediatrics, University of Utah, Salt Lake City, USA (kent.lai@hsc.utah.edu), Eva Morava, M.D., Ph.D., Tamas Kozicz, M.D., Ph.D. Department of Clinical Genomics, Center of Individualized Medicine, Mayo Clinic, Rochester, USA, (Morava-Kozicz.Eva@mayo.edu, Kozicz.Tamas@mayo.edu).
[^]These authors contributed equally

The authors declare no potential conflicts of interest. All authors have read the Journal's authorship agreement and policy on the disclosure of potential conflicts of interest. All authors have read the journal's authorship agreement, and the manuscript has been reviewed and approved by all designated authors. There were no sources of editorial support for the preparation of the manuscript.

alleviate the fatal cardiomyopathy and the associated myopathy. Here we report on left ventricular ejection fraction (LVEF) in 6 individuals with PGM1-CDG. LVEF was pathologically low in most of these individuals and varied between 10–65%. To study the pathobiology of the cardiac disease observed in PGM1-CDG, we constructed a novel cardiomyocyte-specific conditional *Pgm2* gene (mouse ortholog of human *PGM1*) knockout (*Pgm2* cKO) mouse model. Echocardiography studies corroborated a DCM phenotype with significantly reduced ejection fraction and left ventricular dilation similar to those seen in individuals with PGM1-CDG. Histological studies demonstrated excess glycogen accumulation and fibrosis, while ultrastructural analysis revealed Z-disk disarray and swollen/fragmented mitochondria, which was similar to the ultrastructural pathology in the cardiac explant of an individual with PGM1-CDG. In addition, we found decreased mitochondrial function in the heart of KO mice. Transcriptomic analysis of hearts from mutant mice demonstrated a gene signature of DCM. Although proteomics revealed only mild changes in global protein expression in left ventricular tissue of mutant mice, a glycoproteomic analysis unveiled broad glycosylation changes with significant alterations in sarcolemmal proteins including different subunits of laminin-211, which was confirmed by immunoblot analyses. Finally, augmentation of PGM1 in KO mice *via* AAV9-*PGM1* gene replacement therapy prevented and halted the progression of the DCM phenotype.

Introduction

Phosphoglucomutase 1 (PGM1, Fig. 1a) catalyzes the interconversion of glucose-1 phosphate (Glc-1P) and glucose-6 phosphate (Glc-6P), a fundamental step in glycolysis, glycogenesis, and glycogenolysis.[1,2] Early studies showed that PGM1 deficiency resulting from biallelic pathogenic variants in the human *PGM1* gene lead to Glycogen Storage Disorder (GSD) Type 14.[2–4] However, we recently discovered that due to the essential role of PGM1 in monosaccharide activation, PGM1 deficiency also causes a Congenital Disorder of Glycosylation (CDG). PGM1-CDG is characterized by both type I & II glycosylation defects, resulting in both missing and truncated, hypogalactosylated glycans.[3,5–8] In addition to the characteristic liver, musculoskeletal, endocrine, and coagulation system involvement, the most life-threatening complication of PGM1-CDG is the early-onset dilated cardiomyopathy (DCM). About half of the reported PGM1-CDG patients have cardiac presentation, with dilated cardiomyopathy (DCM) being the most common symptom [9]. In addition, restrictive cardiomyopathy was reported in one patient [10]. The degree of left ventricular ejection fraction (LVEF), however, was not reported.

Lately, we have shown that oral D-galactose supplementation in patients with PGM1 deficiency improves serum transferrin hypo-glycosylation, liver function, endocrine abnormalities, and reduces the frequency of hypoglycemic episodes.[11–13] Yet, it is also clear that not all clinical abnormalities, which include the deadly dilated cardiomyopathy and the disease associated myopathy, respond to oral D-galactose. Therefore, the pathophysiology of the disease is likely to be tissue specific.

In this study, we generated and performed extensive structural and functional characterization of a new cardiomyocyte specific conditional *Pgm2* gene (mouse ortholog of human *PGM1*) knockout (KO) mouse model (*Pgm2* cKO). We compared the cardiac

function and pathology of our model to the patient data and a cardiac explant of a PGM1-CDG patient who underwent transplantation due to severe cardiac involvement. Our results not only demonstrated that our animal model recapitulates many of the patient phenotypes, but it also lends new insights into the pathobiology of the cardiac complications in PGM1-CDG through multi-omics analyses. Finally, we investigated the efficacy of *PGM1* augmentation in this novel *Pgm2* cKO mice model. AAV9-*PGM1* gene replacement therapy augmented cardiac PGM1 and prevented and halted the progression of cardiac pathology. The reported data are novel and lay the foundation for future development of a safe, effective therapy to address the unmet medical needs of individuals and their families with PGM1-CDG.

Materials and Methods

Ethics Statement

The patient study was approved by Hospital Institutional Ethics Committee and was performed in accordance with the Declaration of Helsinki. Written informed consent was obtained from the parents of the patients for collection of samples and publication of medical data.

All experiments and procedures with different mouse models were performed in strict adherence to the protocols approved by the IACUC office at the University of Utah.

Natural history study on PGM1-CDG patients

Thirteen patients with genetically confirmed PGM1-CDG were enrolled in the Frontiers in Congenital Disorders of Glycosylation (FCDGC) natural history study at Mayo Clinic. Retrospective and prospective collection of clinical, cardiac, and genetic data was performed according to Institutional Review Board (IRB) protocol *19–005187*. Oral D-Galactose (D-Gal) supplementation was undertaken in patients under a separate IRB protocol *18–007276* for dietary monosaccharide supplementation in CDG. All patients have previously been followed according to standard of care. Written informed consent was obtained from the patients, or the patients' parents, and when possible, verbal assent was obtained from the patients. The demographic, genetic, and cardiac features of the patients are shown in Table 2.

Detailed clinical information on the affected patient with PGM1-CDG prior to heart transplantation

The currently 2-year-old female, the first child of consanguineous parents, was born at term with normal growth parameters. She was diagnosed with pulmonary valve stenosis and dysplastic pulmonary valve at the age of 1.5 months, and was also found to have bifid uvula, and enlarged liver size (2 cm under the costal margin). Balloon dilatation resolved the pulmonary valve stenosis at the age of 3 months. Laboratory studies showed elevated transaminases, increased thyroid stimulating hormone level and decreased coagulation factor activities. Transferrin glycosylation was abnormal and comparable to a mixed type I and type II patterns. She was found to have recurrent hypoglycemia and developed failure to thrive in a 6-month period, necessitating nasogastric feeding. At the age of 6 months,

she was admitted for symptoms of heart failure and an ejection fraction of 54% by echocardiogram. She was diagnosed with dilated cardiomyopathy, mitral valve regurgitation and ventricular non-compaction. Whole exome sequencing was performed in a commercial laboratory and identified a previously reported homozygous missense variant in the *PGM1* gene, c.1544G>A, p.R515Q.[14]

D-galactose treatment was started at the age of 11 months with the improvement of hypoglycemia, coagulation, liver transaminases, and transferrin glycosylation, however, no improvement in cardiac output. Despite aggressive pharmacologic management and mitral valve repair, her ejection fraction continued to decrease, and developed recurrent episodes of cardiopulmonary arrest, and complete heart block. She was treated with Extracorporeal Membrane Oxygenation Treatment (ECMO) and inotropic support for an ejection fraction of 10% and received a pacemaker. She successfully underwent heart transplantation at the age of 12-month.

Echocardiogram in the affected patient prior to heart transplantation

Echocardiogram showed an EF of 73% at the age of 3 months. At the age of 6 months, the patient was admitted in cardiac failure and had an ejection fraction of 54%, which rapidly deteriorated in a week, and progressively decreased to 10% necessitating transplantation at the age of 12 months (Table 1).

The heart explant

Deidentified heart explant sample was donated to the biobank of the Frontiers in CDG Consortium (FCDGC) {Biomarker discovery aim of the natural history study [institutional review board (IRB)]:19005187; https://clinicaltrials.gov/ct2/show/NCT04199000?cond=CDG&draw=2&rank=4}.

Generation of *Pgm2* cKO mice

Pgm2$^{fl/fl}$ mice were constructed at the University of Utah Mutagenesis Generation and Detection Core Facility and the University of Utah Transgenic and Gene Targeting Mouse Core Facility. αMHC-MerCreMer transgenic mice were shared by Dr. Dipayan Chaudhuri M.D., Ph.D., Department of Internal Medicine, University of Utah School of Medicine. These mice were obtained by Dr. Chaudhuri from the Jackson Laboratory (Stock # 005657), which were originally donated by Dr Jeffery D. Molkentin, Cincinnati Children's Hospital. Induction of *Pgm2*-KO was accomplished by oral administration of tamoxifen.

Genotyping

Genomic DNA was prepared from tail clips using the Qiagen Blood and tissue DNA isolation kit (Qiagen) according to the manufacturer's protocol. Approximately 10 ng of the genomic DNA was used for PCR. Genotyping of αMHC-MerCreMer mice was performed using forward, 5′-GGCGTTTTCTGAGCATACCT-3' and reverse 5'-CTACACCAGAGACGGAAATCCA-3' primers. The two sets of primers used for genotyping of *Pgm2*$^{fl/fl}$ mice were: forward, 5′-GCCTGGAAAGGAATGCAAGG-3′; reverse, 5′-CACTGAGGTGCTGTAAGGCA-3′

(*Pgm2*-LoxP-5arm); forward, 5′-TGGGGGTGAGTATTCTGTCATC-3′; reverse, 5′-TCTCCTGTGTCAACCTTCAAAGT-3′ (*Pgm2*-LoxP-3arm).

Echocardiography

Standard transthoracic echocardiogram was performed in the individual affected with PGM1-CDG as part of clinical care. Parasternal short- and long-axis views were used to obtain 2D and M-mode images at different time points of care.

Cardiac function in mice anesthetized with 2% isoflurane (Fluriso) was non-invasively monitored by transthoracic echocardiography using a Visual Sonics Vevo 2100 high-resolution imaging system with a 30 MHz scan head housed at the Small Animal Ultrasound Core Facility at the University of Utah at designated weeks after oral administration of tamoxifen. Parasternal short- and long-axis views were used to obtain 2D and M-mode images. At least 10 independent cardiac cycles per experiment were obtained.

Histological analysis

Hearts were fixed in 10% formalin (PBS buffered), dehydrated, and embedded in paraffin for both human and mice samples. Heart architecture was determined using transverse 5-μm deparaffinized sections stained with H&E. Fibrosis was detected with Masson trichrome staining. Periodic Acid Schiff staining was performed to assess the glycogen deposition on sections of formalin-fixed, heart samples (5-μm in thickness). Tissue processing and histological staining were conducted by the University of Utah ARUP Laboratories Research Histology Core Facility.

Electron microscopy

Tissue processing and microscopy were conducted by the University of Utah Electron Microscopy Core Facility. Mice were anesthetized and fixed by vascular perfusion with 2.5% glutaraldehyde and 1% paraformaldehyde, 6 mM $CaCl_2$, and 2.4% sucrose in 0.1M cacodylate buffer, pH 7.4. Immediately after perfusion, the left ventricle was sliced into strips of 3~5 mm width and immersed in the same fixative for 2 hours at room temperature before being stored at 4 degree celsius. Heart explant received from the donor hospital (preserved in 10 % buffered formalin containing 30% sucrose) was sliced into strips of 3~5 mm width and fixed in glutaraldehyde containing fixative as above. Left ventricular tissue of ~ 1 mm^3 in size was subjected to microwave assisted-fixation and processing protocol using a Pelco Biowave® 36500 (*Ted Pella*, CA) involving sequential steps of 2% osmium post-fixation, 4% uranyl acetate en-bloc staining, serial dehydration in ethanol/acetone, and embedding in epoxy resin Embed 812 (*Electron Microscopy Sciences*, PA). Semithin sections of 0.5-micron thickness were stained with toluidine blue to select the region of interest. Ultrathin sections of 50 nm thickness were poststained with uranyl acetate and lead citrate. Ultra-structures of the heart were examined at 120KV using JOEL JEM 140 equipped with a Gatan Orius digital camera.

RNA isolation, library preparation, and sequencing

The hearts were harvested at three-time points: 2 days, 2 weeks, and 1 month, respectively after full tamoxifen induction. Three hearts from Wild type and *Pgm2* cKO mice were used

for this experiment. The left ventricle tissues were harvested, flash-frozen, and submitted to the Molecular Diagnostics Cores at the Huntsman cancer institute for total RNA isolation. RNA sequencing was performed at the University of Utah Huntsman Cancer Institute (HCI) High-Throughput Genomics Core Facility. RNA concentration was measured with a Qubit RNA BR Assay Kit (*Fisher Scientific*, Cat.no. Q10211). RNA quality was evaluated with an Agilent Technologies RNA ScreenTape Assay (*Agilent Technologies*, CA). Total RNA samples (100–500 ng) were hybridized with Ribo-Zero Gold to substantially deplete cytoplasmic and mitochondrial rRNA from the samples. Stranded RNAseq libraries were prepared as described using the Illumina TruSeq Stranded Total RNA Library Prep Gold kit (*Illumina, Inc.*, CA) with TruSeq RNA UD Indexes (*Illumina, Inc.*, CA). Purified libraries were qualified on an Agilent Technologies 2200 TapeStation using a D1000 ScreenTape assay (*Agilent Technologies*, CA). The molarity of adapter-modified molecules was defined by quantitative PCR using the Kapa Biosystems Kapa Library Quant Kit (*Agilent Technologies*, CA). Individual libraries were normalized to 1.30 nM in preparation for Illumina sequence analysis. Sequencing libraries were chemically denatured and applied to an Illumina NovaSeq flow cell using the NovaSeq XP workflow (*Illumina, Inc.*, CA). Following the transfer of the flow cell to an Illumina NovaSeq 6000 instrument, a 150 × 150 cycle paired-end sequence run was performed using a NovaSeq 6000 S4 reagent Kit v1.5 (*Illumina, Inc.*, CA).

Analysis of RNA-Seq data

The RNA-seq data were analyzed using GSEA to identify gene sets that were enriched in the RNA-Seq data, as compared to the curated gene sets for Hallmark and the canonical pathways of the Molecular signature database (MSigDB). An FDR of < 0.05 was used to identify significantly enriched pathways. [15]

Western blot analysis

For Western blotting of total proteins, left ventricular tissues from KO and Control mice were homogenized in a modified RIPA buffer containing protease and phosphatase inhibitors (*Roche,* CA). Samples were run on an SDS-PAGE gel and transferred to a nitrocellulose membrane (*Li-Cor Biosciences,* NE) using protocols published by our laboratory. Incubation with primary antibodies for PGM1, (HPA024637, *Sigma-Aldrich),* Laminin-211 (PA1–16730, *Invitrogen*), Dystroglycan (11017-AP *Proteintech*), pAkt473 (#9271,Cell signaling Technology), pGsk3β (#9336,Cell signaling Technology), Gapdh (#14C10,Cell signaling Technology) was conducted at a dilution of 1:1000 in antibody dilution buffer (*Li-Cor Biosciences,* NE) as described previously.[16] Primary antibodies were detected with IR dye-conjugated secondary antibodies and visualized by Odyssey Image Analyzer (*Li-Cor Biosciences,* NE). Quantitative analysis of the fluorescence signals was performed by Empiria Studio software (*Li-Cor Biosciences,* NE), and the results were normalized to the corresponding Gapdh abundance detected in the same samples.

Mitochondrial electron transport chain enzyme activities

Cardiac tissue was homogenized in 10 mM Tris-HCl (pH 7.6) using a bead mill homogenizer (Omni International). The activities of mitochondrial complexes I (CI), II (CII), III (CIII), and IV (CIV) were assessed using a spectrophotometric enzyme activity

assay as previously described[17] performed on a FLUOstar Omega spectrophotometric plate reader (BMG). Mitochondrial electron transport chain complex activities were measured and normalized to both citrate synthase (CS) activity and protein concentration. CS is a common readout for mitochondrial mass, and normalization of complex activities to CS activity can reveal actual alterations in activities of the complexes themselves, or alterations in their abundances within the mitochondria, while normalization of complex activities to total protein concentration of the homogenates can potentially reveal alterations in the mitochondrial mass within the tissue.[18]

Proteomics and Glycoproteomics analyses

Pgm2 cKO (n=5) and wildtype (n=3) mouse heart samples after tamoxifen treatment day 30 were lysed in 4% SDS (in 100 mM TEABC) using Bioruptor sonication device. Protein concentrations were estimated by BCA assay as per the manufacturer's instructions (*Thermo Fisher Scientific Inc.,* MA). Glycoproteomics analysis were performed using the method described previously with slight modifications.[19] Detailed protocol will be described in Supplementary Materials.

Proteomics analysis was carried out using LC-MS/MS analysis as previously described [20,21] with some modifications. Detailed protocol will be described in Supplementary Materials. Proteomics data were searched using Sequest search engine in Proteome Discoverer 2.5 against the UniProt Mouse Reviewed protein sequences (21,984 entries) and the glycoproteomics data using the publicly available software pGlyco version 3.0. Statistical analysis was performed using the publicly available MetaboAnalyst computational platform and GraphPad Prism. Two-sample student's t test with unequal group variance was used to define the significance.

Steady-State Metabolomics analysis

Metabolomics analysis was performed at the Metabolomics Core Facility at the University of Utah using GC-MS analysis with an Agilent 5977b GC-MS MSD-HES fit with an Agilent 7693A automatic liquid sampler. Data was collected and analyzed using MassHunter software (*Agilent Technologies,* CA). Metabolite identity was established using a combination of an in-house metabolite library developed using pure purchased standards, the NIST library and the Fiehn library. Detailed methods are provided in the Supplementary Materials.

AAV9-based expression vector

AAV9-*PGM1* harbors a CAG promoter, which was used to drive the codon-optimized full-length human *PGM1* cDNA. The recombinant vector was designed by the Lai Lab and subsequently synthesized at VectorBuilder Inc. (IL) on a fee-for-service basis. A dose of 5×10^{11} vector genomes (VG) was systemically administered through the tail vein, resulting in a mean body weight (BW) adjusted dose of 2.5×10^{13} VG/kg BW.

Statistical Analyses

Data were expressed as the mean ± standard error of the mean (SEM). Statistical analysis included Student t-test, two-way analysis of variance (ANOVA) with Bonferroni post-hoc

correction, or two-way repeated measures of ANOVA with sequential post hoc Bonferroni corrections, or Kolmogorov-Smirnov test, where appropriate, using GraphPad Prism 9 (GraphPad Software).

Results

Natural history studies of PGM1-defient patients with cardiac phenotype

In summary, six individuals with PGM1-CDG had a history of cardiac involvement out of thirteen patients enrolled in Natural History study. The cardiac features of the patients are shown in Table 2. Out of six patients, three patients had significantly decreased LVEF (P1, P5 and P6). All the patients had mild to moderate tricuspid valve insufficiency and four had negative T-waves. Four out of six patients had DCM. All patients received D-Gal therapy, however, no improvement in cardiac function was observed. These results also corroborate previous reports that D-gal therapy is not effective in treating cardiac presentation in PGM1-CDG[10,12,22].

Construction of a new tamoxifen-inducible cardiomyocyte-specific *Pgm2* knockout (*Pgm2* cKO) mouse model

Due to limited research utility of the *constitutive Pgm2* KO mouse model,[16] which is embryonic lethal, we began constructing new tissue-specific *conditional Pgm2* gene-KO mouse model to gain novel insights into the role of *Pgm2* in tissue-specific functions in a living mammal. We generated a new tamoxifen-inducible cardiomyocyte-specific *Pgm2* cKO mouse model. To develop this animal model, we started by constructing the *Pgm2*-floxed animals. Briefly, validated CRISPR-Cas9 RNP complexes along with a long ssDNA donor that inserted two LoxP sites in the introns flanking exon 2 of *Pgm2* (Fig. 1b), were microinjected into the male pronuclei of fertilized C57BL6 embryos. Injected embryos were implanted into *pseudo* pregnant mothers and carried to term. Offspring were genotyped using PCR-Restriction Enzyme Digest assays that identified the insertion of the donor DNA. Animals showing insertion were then sequenced to confirm the perfect insertion of the donor DNA, including functional LoxP sites (Fig. 1b). Homozygous *Pgm2*-floxed animals were subsequently obtained by crossing heterozygous parents. We crossed the homozygous *Pgm2*-floxed animals to mice that harbored the alpha-MHC-MerCreMer (αMHC-MerCreMer) transgene, which has the mouse cardiac-specific alpha-myosin heavy chain promoter (αMHC or alpha-MHC; Myh6) directing the expression of a tamoxifen-inducible Cre recombinase (MerCreMer) in juvenile and adult cardiac myocytes.[23] These αMHC-MerCreMer transgenic mice allow the creation of bi-transgenic mice for Cre-lox studies of temporally regulated deletion of loxP-flanked targeted genes in cardiac tissues/cells. Once the progeny with the desired combined genotypes were obtained and confirmed, we began oral treatment of the animals with tamoxifen (35mg/kg body weight for 5 days) at approximately 4 weeks of age to induce the excision of exon 2 of the *Pgm2* alleles in cardiomyocytes. Multiple factors led us to choose the 4-week time point, and they include, but are not limited to, (a) Since many PGM1-CDG patients develop cardiac defects in early life (younger than 2 years old), a time point soon after weaning age (3 weeks in mice) should match well with the patient condition. (b) Cardiomyocytes stop proliferating at this

point, which will enable us to avoid the dilution issue and ensure long-lasting effects of subsequent AAV9-PGM1 treatment.

We chose oral administration of tamoxifen because it was shown that intraperitoneal administration of tamoxifen could cause transient cardiomyopathy in mice.[24] In addition, the dosage we selected was far below the 75mg/kg (maximum dosage) recommended by the Jackson Laboratory to minimize undue cardiotoxicity in our mice. Deletion of *Pgm2* in the heart was confirmed by immunoblots on heart tissue using anti-human PGM1 antibody which cross-reacts with the mouse ortholog. Results demonstrated over 95% reduction in Pgm2 protein in *Pgm2*-cKO hearts (Fig. 1c).

Pgm2 cKO mice develop dilated cardiomyopathy (DCM)

As individuals with PGM1-CDG develop dilatated cardiomyopathy,[7] we first examined the morphology of the heart in *Pgm2* cKO mice and littermate controls. We found significantly dilated left ventricles already visible at 4 weeks after tamoxifen feeding in *Pgm2* cKO mice, whereas wild-type mice displayed normal cardiac size (Fig. 2a). Echocardiographic analysis revealed the development of dilated cardiomyopathy (DCM) in *Pgm2* cKO mice as evidenced by decreased fractional shortening (FS), ejection fraction (EF) and increased left ventricular end-diastolic internal dimensions (LVID-d) as early as 2 weeks after tamoxifen feeding and continue to worsen with age. A representative set of results collected at 16 weeks post-tamoxifen is shown in Fig. 2b. In addition, KO mice also displayed an increase in the early to late ventricular filling velocities (E/A) ratio that was measured across the mitral valve (Fig. 2b).

Additional signs of DCM were revealed at the histological levels. At low magnification, hematoxylin, and eosin (H & E) staining of WT and *Pgm2* cKO hearts revealed enlarged right and left ventricular chambers with thinner walls 16 weeks after tamoxifen feeding (Fig. 2c). To assess how closely these and latter findings resemble human patient phenotypes, we included results from a transplanted heart from a young patient with PGM1-CDG. Fibrosis was present in the hearts of *Pgm2* cKO mice as well as in the heart of the PGM1-CDG patient (Fig. 2d). Similarly, hearts from the *Pgm2* cKO mice and the PGM1-CDG patient exhibited enhanced glycogen accumulation as evidenced by positive PAS staining (Fig. 2e).

We used transmission electron microscopy to evaluate the ultrastructure of *Pgm2* cKO hearts as well as a heart from a PGM1-CDG patient. As shown in Figs. 2f–g, we observed disrupted myofibrillar organization, reduced mitochondrial matrix density, and fragmented mitochondrial cristae in *Pgm2* cKO mice as early as two weeks after tamoxifen feeding. Similarly, loss of cardiomyocyte integrity and abnormal mitochondria with less organized cristae were observed in the heart of the PGM1-CDG patient (Fig. 2f, g).

Transcriptomic analysis of *Pgm2* cKO hearts reveals a biphasic metabolic response consistent with a progressive mitochondrial demise

As our analyses above indicated that our mouse model recapitulates the patient cardiac phenotypes, we proceeded to conduct more in-depth omics analyses of our model as a first step to unveil the underlying molecular pathophysiology of the cardiac phenotypes. We adopted a time-course multi-omics strategy as depicted in Fig. 3a where we examined

cohorts of 4-wee-kold mutant and wildtype male animals at different time points after tamoxifen induction.

We used unbiased RNAseq analysis to investigate the transcriptional changes that occur in *Pgm2* cKO mice before, during and after the establishment of DCM. We studied cohorts of 4-week-old wildtype and *Pgm2* cKO mice at three different time points (2, 14 and 30 days) after tamoxifen feeding. At two days post-tam, only 41 upregulated and 67 down-regulated genes were identified between the *Pgm2* cKO and control hearts. The number of up-regulated genes increased to 308 and 1058 at day 14 and day 30, respectively, while the number of the down-regulated genes increased to 247 and 383 at the same time points (Fig. 3b). As depicted in Fig. 3c, we initially observed a compensatory increase in the expression of genes involved in fatty acid oxidation, oxidative phosphorylation, glycolysis and TCA cycle at 2 and 14 days post-tamoxifen in *Pgm2* cKO mice, which was subsequently reversed at 30 days post-tamoxifen. This is a unique change as other gene signatures known to be activated during DCM such as E2F/TP53[25] were reduced at 2 days post-tamoxifen but up-regulated at 14 and 30 days post-tamoxifen. These results are consistent with the development of a progressive energetic demise in the hearts of *Pgm2* cKO mice.

Proteomics analysis of *Pgm2* cKO hearts demonstrates altered abundance of proteins involved in energy and lipid metabolism.

We performed a quantitative proteomics analysis of five *Pgm2* cKO and three WT mouse hearts using a tandem mass tag (TMT)-based multiplexing strategy coupled to LC-MS/MS. Multiplexed proteomics study identified a total of 4,396 proteins with 68,599 peptides. The volcano plot shows the distribution of protein expression (Fig. 4A). We found changes in global protein expression in hearts from *Pgm2* cKO mice. Several of the significantly changing proteins (p-value <0.05) are known to be involved in lipid and energy metabolism. We found several proteins that showed >50% upregulation and <0.05 p-value including alpha-1B-glycoprotein, corticosteroid-binding globulin (Cbg/Serpina6), complement factor D, protein S100-A1 and mitochondrial cytochrome c oxidase subunit 5A. The protein level of Pgm1 was reduced in all *Pgm2* cKO samples by ~ 80% as compared to WT samples. We found several proteins with >50% downregulation and <0.05 p-value including mitochondrial NAD(P) transhydrogenase (Nnt), alpha-1-antitrypsin 1, mitochondrial D-2-hydroxyglutarate dehydrogenase (D2hgdh), C8b, C8g and epidermal growth factor receptor (Egfr). The expression level of electron transport chain complexes was comparable between *Pgm2*-KO and WT mouse hearts. The expression pattern of several of the most upregulated and downregulated proteins across both group of samples are shown in a heatmap (Fig. 4B). The distributions for Pgm1, Nnt, D2hgdh and Cbg in all *Pgm2*-cKO and WT mouse heart samples are shown in Fig. 4C as box plots. Complete list of significantly changing proteins (p-value <0.05) interrogated with the fold-change can be found as Supplementary Materials deposited to PRIDE (Accession number pending).

Glycoproteomics analysis of *Pgm2* cKO hearts unveils qualitative and quantitative changes in glycoproteins essential for cardiomyocyte functions

We focused the glycoproteomic analyses of *Pgm2* cKO mouse heart samples 30 days after tamoxifen treatment. In our global glycoproteomics study of mouse hearts, we identified

and quantified 1,640 individual N-glycopeptides with 147 unique N-glycan compositions on 440 glycosylation sites of 271 glycoproteins. Our results revealed widespread quantitative alterations in glycosylation in *Pgm2* cKO hearts involving diverse glycans ranging from high-mannose and hybrid/complex to sialylation and fucosylation. Significant glycosylation changes ($p < 0.05$) were observed in 213 unique N-glycopeptides derived from 71 distinct glycoproteins, of which 171 glycopeptides derived from 56 glycoproteins were reduced in *Pgm2* cKO compared to WT (Fig. 4D). Heatmap of all quantified 1,640 glycopeptides in *Pgm2* cKO and WT mouse hearts is shown in Fig. 4E. Partial Least Squares Discriminant Analysis (PLS-DA) revealed separation of *Pgm2* cKO and WT mouse hearts at the glycopeptide level (Fig. 4F).

The most significantly increased glycopeptide (~22-fold) containing a complex glycan (Hex5HexNAc4NeuGc2Fuc1) on a peptide derived from corticosteroid-binding globulin (Cbg). The most significantly downregulated glycopeptides included Hex5HexNAc4NeuGc2 and Hex5HexNAc4NeuGc3 glycans on the same peptide from complement factor 9. Remarkably, of the 213 glycopeptides in *Pgm2* cKO hearts that were significantly altered, over one-third (74 glycopeptides) were derived from multiple glycosylation sites of various subunits of laminin. Among these 74 glycopeptides, 71 were downregulated. Aberrant glycosylation was detected in 28 glycopeptides from the alpha-2 subunit (Lama2), 9 glycopeptides from the alpha-4 subunit (Lama4), 1 glycopeptide from the alpha-5 subunit (Lama5), 4 glycopeptides from beta-1 subunit (Lamb1), 10 glycopeptides from the beta-2 subunit (Lamb2) and 22 glycopeptides from gamma-1 subunit (Lamc1) of the laminin protein family (Fig. 4G). The expression pattern of several of the dysregulated glycopeptides derived from these subunits of laminin family across both group of samples is shown as a heatmap (Fig. 4H). The distribution of some of the most significantly altered glycopeptides from laminin family in all *Pgm2* cKO and WT mouse heart samples is shown in Fig. 4I as box plots. Significant glycosylation changes were also detected for sarcoglycan and biglycan. A complete list of significantly changing proteins (p-value <0.05) along with their fold-change values can be found as Supplementary Materials deposited to PRIDE (Accession number pending).

Laminin-211 heterotrimer and its downstream interaction targets are altered in *Pgm2* cKO hearts

In mouse cardiomyocytes, Laminin-211, a heterotrimer composed of the alpha 2 (Lama2), beta 1 (Lamb1) and gamma 1 (Lamc1) subunits, interacts with α-dystroglycan and integrin α7β1 and plays important roles in myofibril functions and myocyte survival, respectively[26,27]. To the best of our knowledge, natural variants in the genes that encode the two subunits, beta 1 and gamma 1 of Laminin-211 do not result in any cardiac dysfunctions in patients. In addition, deleterious *LAMA2* gene variants in humans can lead to LAMA2 muscular dystrophy (LAMA2-MD), which can also include cardiac involvement; predominantly dilated cardiomyopathy, right bundle branch block (RBBB), mitral valve prolapse and variable other changes in cardiac function.[28,29]

To study the role of mis-glycosylated alpha-2 subunit (Lama2) of Laminin-211 protein in cardiac function of *Pgm2* cKO mouse heart 30 days after tamoxifen induction, we analyzed

the abundance of Laminin-211 and its downstream targets using Western blot analysis. We found that Laminin-211 protein and Laminin binding protein abundance was significantly reduced in the *Pgm2* cKO mouse hearts (Fig. 4J). Interestingly, we did not see any significant changes in the α-dystroglycan abundance. Given the strong association between α2 subunit of Laminin-211 and integrin α7β1, we performed protein expression analysis on Pi3k/Akt signaling pathway to examine whether aberrant glycosylation of α2 subunit (Lama2) of Laminin-211 impairs its interaction with integrins and downstream Pi3k/Akt survival signaling in the *Pgm2* cKO hearts. Western blot analysis revealed significant reduced expression of phospho- Akt (Ser473) and phospho-Gsk3β molecules as shown in Fig. 4J.

Steady-State Metabolomics analysis in *Pgm2* cKO hearts indicates disturbances in energy metabolism

Our previous tracer metabolomic studies in PGM1-CDG patient-derived dermal fibroblasts pointed towards a disturbance of TCA cycle metabolites.[13] These data suggested that glucose is being redirected away from TCA cycle and towards other pathways, which results in impaired energy metabolism. In this study, we carried out steady state cardiac metabolomics analysis in the *Pgm2* cKO mice at day 30 post-tamoxifen and showed a reduction in TCA cycle metabolites succinate, fumarate and aspartate and the accumulation of lactate, a known marker of mitochondrial energy failure, suggesting reduced flux through the TCA cycle (Fig. 5b). We also measured the specific activity of the individual complexes of the mitochondrial respiratory chain by a spectrophotometric assay. We found decreased Complex III activity (~25%) in the hearts of the *Pgm2* cKO compared to WT littermates 30 days post-tamoxifen (Fig. 5c). Activities of the other complexes on the mitochondrial electron transport chain were comparable between the groups (Fig. 5c).

AAV9-*PGM1* gene replacement therapy prevents the manifestation DCM in *Pgm2* cKO mice

To test the hypothesis that augmentation of PGM1 expression in cardiomyocytes would prevent the development of dilated cardiomyopathy, we treated cohorts of wildtype and *Pgm2* cKO mice at 4 weeks of age with AAV9-*PGM1* (2.5 E+13 vg/kg) by tail vein injection, prior to tamoxifen feeding (Fig. 6a).

As shown in Figs. 6b & c, echocardiography measurement of the untreated *Pgm2* cKO mice showed a significant reduction in ejection fraction (EF) and fractional shortening (FS), increase in LV mass, and a larger left ventricular internal diameter at systole compared to the treated group. Augmentation of PGM1 activity in the mice prior to tamoxifen feeding prevented the reduction in EF and FS, increase in LV mass or LV internal diameter over the period of 4 months after treatment. Importantly, the treatment also avoided the accumulation of excess glycogen and fibrosis (Fig. 6d).

A single intravenous injection of AAV9 *PGMI* halts the progression DCM in *Pgm2* cKO mice

To test the efficacy of AAV9-*PGM*1 gene replacement therapy in a more clinically relevant context, we induced *Pgm2* cKO at 4 weeks of age and performed echocardiography regularly until we detected the deterioration in cardiac functions. We then randomized the animals and treat a selected group with AAV9-h*PGM1* (2.5 E+13 vg/kg) and followed them

by monitoring their cardiac function by echocardiography for another 15 weeks (Fig. 7a). We chose 2.5E+13 vg/kg for this and the above studies because it has been shown that such dosage can prevent and reverse heart failure in rodent models of Barth Syndrome and other cardiovascular diseases.[30–33] Moreover, we showed that such dosage restored the expression of PGM1 close to those at wild-type (Fig. 7a), which should avoid lack of efficacy due to insufficient expression or potential toxicity due to over-expression of PGM1.

Hearts were collected at the end point and subjected to molecular and histological studies. As shown in Fig. 7b, echocardiography follow-ups at different time points demonstrated progressive deterioration of cardiac function in the cohort without treatment. Importantly, the treated group did not develop further worsening of the cardiac functions and exhibited no excess accumulation of glycogen or fibrosis (Fig. 7c).

Discussion

Cardiac dysfunction in the form of dilated cardiomyopathy (DCM) is the most severe, progressive presentation in PGM1-CDG, the third most common type of Congenital Disorders of Glycosylation (CDG). It is present in about half of the patients many of whom die of cardiac arrest at an early age.[7,34] The pathogenic mechanism that promote heart dysfunction in PGM1 deficiency is not clear.

Six of the thirteen individuals with genetically confirmed PGM1-CDG enrolled in the FCDGC natural history study at Mayo Clinic had a history of cardiac involvement. Three for the six individuals presented with significantly decreased LVEF, and all individuals had mild to moderate tricuspid valve insufficiency (Table 2). All patients received D-Gal therapy, however, no improvement in cardiac function was observed (Table 2). These results also corroborate previous reports that D-gal therapy is not effective in treating cardiac presentation in PGM1-CDG[10,12,22].

To study the pathobiology of cardiac disease in individuals with PGM1-CDG, we constructed cardiomyocyte-specific conditional *Pgm2* (mouse ortholog of human *PGM1*) gene knockout mice (*Pgm2* cKO) mice. Using echocardiography (Fig. 2b), we corroborated a phenotype of DCM with significantly reduced ejection fraction as well as left ventricular dilation indicating the presence of contractile defects similar to those seen in individuals with PGM1-CDG. Histological studies revealed glycogen accumulation and fibrosis (Fig 2d, e). Ultrastructural analysis of heart tissues from *Pgm2* cKO mice and the human explant revealed Z-disk disarray, swollen/fragmented mitochondria. We also saw thickening in the heart of PGM1-CDG patient (Fig. 2f, g) upon macroscopic examination.

Transcriptomic analysis of hearts from the *Pgm2* cKO mice demonstrated a gene signature of DCM with characteristic changes in the E2F/TP53[25] pathway. The bi-phasic changes of genes involved in fatty oxidation and OXPHOS (Fig. 3c) were among the first in this study to suggest that perturbation of energy metabolism may also play a role in DCM in PGM1-CDG. This notion has been corroboarted by proteomic analyses revealing that some of the top differentially expressed proteins resided in the mitochondria (Fig. 4A–C, Supplimentary materials). Further, we demonstrated a reduction in TCA cycle metabolites

succinate and fumarate, as well as the accumulation of lactate (Fig. 5b), a known marker of mitochondrial energy failure, suggesting reduced flux through the TCA cycle. Thus, the current results were similar to our previous tracer studies on patient fibroblasts, demonstrating the depletion of TCA cycle metabolites fumarate, malate, citrate, isocitrate and aspartate.[13] More importantly, we demonstrated a 25% reduction of mitochondrial complex III activity in the hearts of the *Pgm2* cKO mice (Fig. 5c) establishing a role for energy metabolism in the DCM phenotype of these mice.

Due to the glycosylation defects detected in individuals with PGM1-CDG[7] and the Pgm2-deficient mouse model[16], we believe that aberrant glycosylation of proteins crucial for cardiac function could contribute to the DCM phenotype. Assessing the glycoproteomic profile of left ventricular tissue of *Pgm2* cKO mice, we showed significant glycosylation defects in sarcolemmal proteins including laminin family, sarcoglycans and biglycan (Fig. 4G–I, Supplementary Materials) – glycoproteins that are crucial for normal cardiac functions. In fact, clinical manifestations of *LAMA2* muscular dystrophy (*LAMA2*-MD) includes cardiac involvement; predominantly dilated cardiomyopathy, right bundle branch block (RBBB), mitral valve prolapse and variable other changes in cardiac function.[35–39] Moreover, it should be noted that dilated cardiomyopathy, rhythm abnormalities, valve abnormalities, proximal muscle weakness, elevated creatine kinase (CK) levels, and normal intelligence are fully overlapping symptoms between *LAMA2*-MD and PGM1-CDG. Furthermore, laminin-211 is associated with the dystrophin-associated glycoprotein complex (DGC) and the sarcolemma and anchors the muscle cell membrane to the extracellular matrix (ECM) and have essential roles in cardiomyocyte health and functions.[40] Loss of functional laminin family allows contracting myofibers to detach from the ECM, activate signaling pathways and undergo apoptosis.[41] Therefore, mis-glycosylation of the subunits of laminin family can potentially affects its binding to dystroglycan or integrin α7β1.[35,42] As shown in Fig.4J, *Pgm2* cKO hears also showed reduced protein abundance of Laminin-211 and its downstream signaling molecules. Therefore, we believe that aberrant glycosylation of α2 subunit (Lama2) of Laminin-211 adversely affects its self-assembly and stability, which in turn alters the interaction with integrin α7β1 and/or α-dystroglycan in our mouse model. As such interactions are critical for cardiomyocyte survival and functions, the altered interactions in the *Pgm2* cKO hearts thus contribute to the development of DCM in *Pgm2* cKO mice. To date, the implications of altered laminin glycosylation on other sarcolemmal proteins and in cardiac function has not been evaluated and our model offers an opportunity to study this further. Collectively, not only does our mouse model recapitulate the cardiac phenotypes of individuals with PGM1-CDG, but our deep structural and functional phenotyping also supports the overarching hypothesis that altered glycosylation alone cannot fully explain the pathobiology of cardiac symptoms in PGM1-CDG patients as secondary mitochondrial dysfunction and metabolic disturbances could also contribute to the pathobiology of DCM in PGM1-CDG.

Recently, we reported on successful oral D-galactose supplementation in a growing cohort of patients with PGM1 deficiency, with improved serum transferrin hypo-glycosylation, liver function, endocrine abnormalities, and reduced the frequency of hypoglycemic episodes. However, the cardiac and the myopathy-related phenotypes were not corrected by this dietary therapy.[7,11] Therefore, discovering novel therapies for cardiac and the myopathy-

related phenotypes remains an unmet medical need in PGM1-CDG. This has prompted us to apply AAV-*PGM1* gene replacement *in vivo*. We have established the cause-and-effect relationships between PGM1 deficiency and abnormal protein glycosylation/energy metabolism, as well as the subsequent impaired cardiac functions (Fig. 6). Additionally, we demonstrated the efficacy of AAV-*PGM1* gene replacement in halting the progression of the DCM phenotype in *Pgm2* cKO mice (Fig. 7). As AAV9-based vectors can target other organs that are affected in patients with PGM1-CDG, this experimental gene replacement therapy has the potential to address other tissue-specific disease phenotypes such as myopathy.

We report on deep structural and functional phenotyping of a new *Pgm2* cKO mice. The described cardiac presentations in the *Pgm2* cKO mice recapitulate many of the cardiac pathology seen in individuals with PGM1-CDG. We also found comparable (ultra)structural alterations in *Pgm2 cKO* mice and in heart explants of an individual with PGM1-CDG. Finally, AAV9-*PGM1* gene replacement therapy prevented and halted the progression of the DCM phenotype in *Pgm2 cKO* mice. These studies not only further our understanding of the pathobiology of DCM in individuals with PGM1-CDG but provide potential novel therapeutic avenues to treat the hereto therapy resistant life-threatening DCM in individuals with PGM1-CDG.

Brief Commentary

In this study, we report the cardiac pathology of a child with phosphoglucomutase I (PGM1) deficiency who underwent heart transplantation for rapidly deteriorating cardiac disease early after birth. In addition, we describe the generation of a novel mouse model of PGM1-CDG and through our comprehensive phenotypic characterization of this murine model, we pinpoint that mis-glycosylation of laminin subunits and altered energy metabolism as likely causes of the dilated cardiomyopathy (DCM) phenotype. The identification of a new role of glycosylation of intermediate filament in DCM development is highly significant as it adds a new link between glycosylation and cardiac functions. Last but not least, we show that we can correct the cardiac phenotype using an AAV vector expressing the wild type *PGM1* cDNA, thus laying the foundation for a novel therapy to address the unmet medical needs of the patients.

Supplementary Material

Refer to Web version on PubMed Central for supplementary material.

Acknowledgements

We want to acknowledge the scientific and technical support, which include the use of equipment and instrument from the following University of Utah Core Facilities:

1. University of Utah Mutagenesis Generation and Detection Core Facility (Director: Crystal Davey, Ph.D.)
2. University of Utah Transgenic and Gene Targeting Mouse Core Facility (Directors: Kyle O'Connor and Crystal Davey, Ph.D.)
3. University of Utah Electron Microscopy Core Facility (Director: David M. Belnap, Ph.D.)
4. Small Animal Ultrasound Core Facility at the University of Utah (Director: Kevin Whitehead, M.D.)

5. Molecular Diagnostics Cores at the Huntsman cancer institute for Total RNA isolation (Director: Nieca Bronson, M.S.)

6. University of Utah Huntsman Cancer Institute (HCI) High-Throughput Genomics Core Facility (Director: Brian K. Dalley, Ph.D.)

7. HCI Bioinformatic Analysis Core Facility (Director: David Nix, Ph.D.)

8. Metabolomics Core Facility at the University of Utah (Director: James Cox, Ph.D.)

We also would like to thank Dr. Dipayan Chaudhuri M.D., Ph.D. for sharing his αMHC-MerCreMer transgenic mice.

Funding

A.P. was funded by a grant from the NCI to the Mayo Clinic Comprehensive Cancer Center (NCI P30 CA15083).

S.B. is supported by the National Heart, Lung, and Blood Institute (NHLBI) grant R01HL149870-01A1, the National Institute of Diabetes and Digestive and Kidney Diseases (NIDDK) grant R01DK128819-01), and University of Utah Office of Vice-President of Research seed grant.

E.M. & T.K. are supported by the grant entitled *Frontiers in Congenital Disorders of Glycosylation* (1U54NS115198-01) from the National Institute of Neurological Diseases and Stroke (NINDS) and the National Center for Advancing Translational Sciences (NCATS), National Institute of Child Health and Human Development and the Rare Disorders Clinical Research Network (RDCRN), at the National Institute of Health.

K.L. is supported by the Eunice Kennedy Shriver National Institute of Child Health and Human Development grants (R01HD089933, R21HD104056), *Frontiers in Congenital Disorders of Glycosylation (FCDGC) Feasibility and Pilot Grant*, University of Utah College of Pharmacy and Center for Genomic Medicine Therapeutic Catalyst Grant, and University of Utah Office of Vice-President of Research seed grant.

References

1. Beamer L. Mutations in hereditary phosphoglucomutase 1 deficiency map to key regions of enzyme structure and function. Journal of Inherited Metabolic Disease. 2015;38(2):243–256. [PubMed: 25168163]
2. Stojkovic T, Vissing J, Petit F, et al. Muscle glycogenosis due to phosphoglucomutase 1 deficiency. N Engl J Med. 2009;361(4):425–427. [PubMed: 19625727]
3. Ondruskova N, Honzik T, Vondrackova A, et al. Glycogen storage disease-like phenotype with central nervous system involvement in a PGM1-CDG patient. Neuroendocrinology Letters. 2014;35(2):137–141. [PubMed: 24878975]
4. Voermans NC, Preisler N, Madsen KL, et al. PGM1 deficiency: Substrate.use during exercise and effect of treatment with galactose. Neuromuscular Disorders. 2017;27(4):370–376. [PubMed: 28190645]
5. Kucukcongar A, Tumer L, Ezgu FS, et al. A Case with Rare Type of Congenital Disorder of Glycosylation: Pgm1-Cdg. Genetic Counseling. 2015;26(1):87–90. [PubMed: 26043514]
6. Perez B, Medrano C, Ecay MJ, et al. A novel congenital disorder of glycosylation type without central nervous system involvement caused by mutations in the phosphoglucomutase 1 gene. Journal of Inherited Metabolic Disease. 2013;36(3):535–542. [PubMed: 22976764]
7. Tegtmeyer LC, Rust S, van Scherpenzeel M, et al. Multiple Phenotypes in Phosphoglucomutase 1 Deficiency. New England Journal of Medicine. 2014;370(6):533–542. [PubMed: 24499211]
8. Timal S, Hoischen A, Lehle L, et al. Gene identification in the congenital disorders of glycosylation type I by whole-exome sequencing. Human Molecular Genetics. 2012;21(19):4151–4161. [PubMed: 22492991]
9. Altassan R, Radenkovic S, Edmondson AC, et al. International consensus guidelines for phosphoglucomutase 1 deficiency (PGM1-CDG): Diagnosis, follow-up, and management. J Inherit Metab Dis. 2021;44(1):148–163. [PubMed: 32681750]
10. Donoghue SE, White SM, Tan TY, et al. Galactose treatment of a PGM1 patient presenting with restrictive cardiomyopathy. JIMD Rep. 2021;57(1):29–37. [PubMed: 33473337]

11. Morava E. Galactose supplementation in phosphoglucomutase-1 deficiency; review and outlook for a novel treatable CDG. Molecular Genetics and Metabolism. 2014;112(4):275–279. [PubMed: 24997537]
12. Wong SYW, Gadomski T, van Scherpenzeel M, et al. Oral D-galactose supplementation in PGM1-CDG. Genetics in Medicine. 2017;19(11):1226–1235. [PubMed: 28617415]
13. Radenkovic S, Bird MJ, Emmerzaal TL, et al. The Metabolic Map into the Pathomechanism and Treatment of PGM1-CDG. Am J Hum Genet. 2019.
14. Conte F, Morava E, Bakar NA, et al. Phosphoglucomutase-1 deficiency: Early presentation, metabolic management and detection in neonatal blood spots. Mol Genet Metab. 2020;131(1-2):135–146. [PubMed: 33342467]
15. Krämer A, Green J, Pollard J, et al. Causal analysis approaches in Ingenuity Pathway Analysis. Bioinformatics. 2014;30(7):923–930. [PubMed: 24227677]
16. Balakrishnan B, Verheijen J, Lupo A, et al. A novel phosphoglucomutase-deficient mouse model reveals aberrant glycosylation and early embryonic lethality. J Inherit Metab Dis. 2019;42(5):998–1007. [PubMed: 31077402]
17. Rodenburg RJ. Biochemical diagnosis of mitochondrial disorders. J Inherit Metab Dis. 2011;34(2):283–292. [PubMed: 20440652]
18. Emmerzaal TL, Preston G, Geenen B, et al. Impaired mitochondrial complex I function as a candidate driver in the biological stress response and a concomitant stress-induced brain metabolic reprogramming in male mice. Transl Psychiatry. 2020;10(1):176. [PubMed: 32488052]
19. Budhraja R, Saraswat M, De Graef D, et al. N-glycoproteomics reveals distinct glycosylation alterations in NGLY1-deficient patient-derived dermal fibroblasts. J Inherit Metab Dis. 2022.
20. Mun DG, Renuse S, Saraswat M, et al. PASS-DIA: A Data-Independent Acquisition Approach for Discovery Studies. Anal Chem. 2020;92(21):14466–14475. [PubMed: 33079518]
21. Chavan S, Mangalaparthi KK, Singh S, et al. Mass Spectrometric Analysis of Urine from COVID-19 Patients for Detection of SARS-CoV-2 Viral Antigen and to Study Host Response. Journal of proteome research. 2021;20(7):3404–3413. [PubMed: 34077217]
22. Radenkovic S, Bird MJ, Emmerzaal TL, et al. The Metabolic Map into the Pathomechanism and Treatment of PGM1-CDG. Am J Hum Genet. 2019;104(5):835–846. [PubMed: 30982613]
23. Sohal DS, Nghiem M, Crackower MA, et al. Temporally regulated and tissue-specific gene manipulations in the adult and embryonic heart using a tamoxifen-inducible Cre protein. Circulation research. 2001;89(1):20–25. [PubMed: 11440973]
24. Koitabashi N, Bedja D, Zaiman AL, et al. Avoidance of transient cardiomyopathy in cardiomyocyte-targeted tamoxifen-induced MerCreMer gene deletion models. Circulation research. 2009;105(1):12–15. [PubMed: 19520971]
25. Chen SN, Lombardi R, Karmouch J, et al. DNA Damage Response/TP53 Pathway Is Activated and Contributes to the Pathogenesis of Dilated Cardiomyopathy Associated With LMNA (Lamin A/C) Mutations. Circulation research. 2019;124(6):856–873. [PubMed: 30696354]
26. Hochman-Mendez C, Curty E, Taylor DA. Change the Laminin, Change the Cardiomyocyte: Improve Untreatable Heart Failure. Int J Mol Sci. 2020;21(17).
27. Shaw L, Sugden CJ, Hamill KJ. Laminin Polymerization and Inherited Disease: Lessons From Genetics. Front Genet. 2021;12:707087.
28. Sarkozy A, Foley AR, Zambon AA, et al. LAMA2-Related Dystrophies: Clinical Phenotypes, Disease Biomarkers, and Clinical Trial Readiness. Front Mol Neurosci. 2020;13:123. [PubMed: 32848593]
29. Prandini P, Berardinelli A, Fanin M, et al. LAMA2 loss-of-function mutation in a girl with a mild congenital muscular dystrophy. Neurology. 2004;63(6):1118–1121. [PubMed: 15452315]
30. Wang S, Li Y, Xu Y, et al. AAV Gene Therapy Prevents and Reverses Heart Failure in a Murine Knockout Model of Barth Syndrome. Circulation research. 2020;126(8):1024–1039. [PubMed: 32146862]
31. Bish LT, Morine K, Sleeper MM, et al. Adeno-associated virus (AAV) serotype 9 provides global cardiac gene transfer superior to AAV1, AAV6, AAV7, and AAV8 in the mouse and rat. Hum Gene Ther. 2008;19(12):1359–1368. [PubMed: 18795839]

32. Garcia-Manzanares M, Tarazon E, Ortega A, et al. XPO1 Gene Therapy Attenuates Cardiac Dysfunction in Rats with Chronic Induced Myocardial Infarction. J Cardiovasc Transl Res. 2020;13(4):593–600. [PubMed: 31768947]
33. Wang J, Shi Q, Wang Y, et al. Gene Therapy With the N-Terminus of Junctophilin-2 Improves Heart Failure in Mice. Circulation research. 2022;130(9):1306–1317. [PubMed: 35317607]
34. Arimura T, Inagaki N, Hayashi T, et al. Impaired binding of ZASP/Cypher with phosphoglucomutase 1 is associated with dilated cardiomyopathy. Cardiovasc Res. 2009;83(1):80–88. [PubMed: 19377068]
35. Nguyen Q, Lim KRQ, Yokota T. Current understanding and treatment of cardiac and skeletal muscle pathology in laminin-alpha2 chain-deficient congenital muscular dystrophy. Appl Clin Genet. 2019;12:113–130. [PubMed: 31308722]
36. Gavassini BF, Carboni N, Nielsen JE, et al. Clinical and molecular characterization of limb-girdle muscular dystrophy due to LAMA2 mutations. Muscle Nerve. 2011;44(5):703–709. [PubMed: 21953594]
37. Marques J, Duarte ST, Costa S, et al. Atypical phenotype in two patients with LAMA2 mutations. Neuromuscul Disord. 2014;24(5):419–424. [PubMed: 24534542]
38. Abdel Aleem A, Elsaid MF, Chalhoub N, et al. Clinical and genomic characteristics of LAMA2 related congenital muscular dystrophy in a patients' cohort from Qatar. A population specific founder variant. Neuromuscul Disord. 2020;30(6):457–471. [PubMed: 32444167]
39. Nelson I, Stojkovic T, Allamand V, et al. Laminin alpha2 Deficiency-Related Muscular Dystrophy Mimicking Emery-Dreifuss and Collagen VI related Diseases. J Neuromuscul Dis. 2015;2(3):229–240. [PubMed: 27858741]
40. Langenbach KJ, Rando TA. Inhibition of dystroglycan binding to laminin disrupts the PI3K/AKT pathway and survival signaling in muscle cells. Muscle Nerve. 2002;26(5):644–653. [PubMed: 12402286]
41. Packer D, Martin PT. Micro-laminin gene therapy can function as an inhibitor of muscle disease in the dy(W) mouse model of MDC1A. Mol Ther Methods Clin Dev. 2021;21:274–287. [PubMed: 33869655]
42. Moll J, Barzaghi P, Lin S, et al. An agrin minigene rescues dystrophic symptoms in a mouse model for congenital muscular dystrophy. Nature. 2001;413(6853):302–307. [PubMed: 11565031]
43. Perales-Clemente E, Liedtke K, Studinski A, et al. A new D-galactose treatment monitoring index for PGM1-CDG. J Inherit Metab Dis. 2021;44(5):1263–1271. [PubMed: 34043239]

a

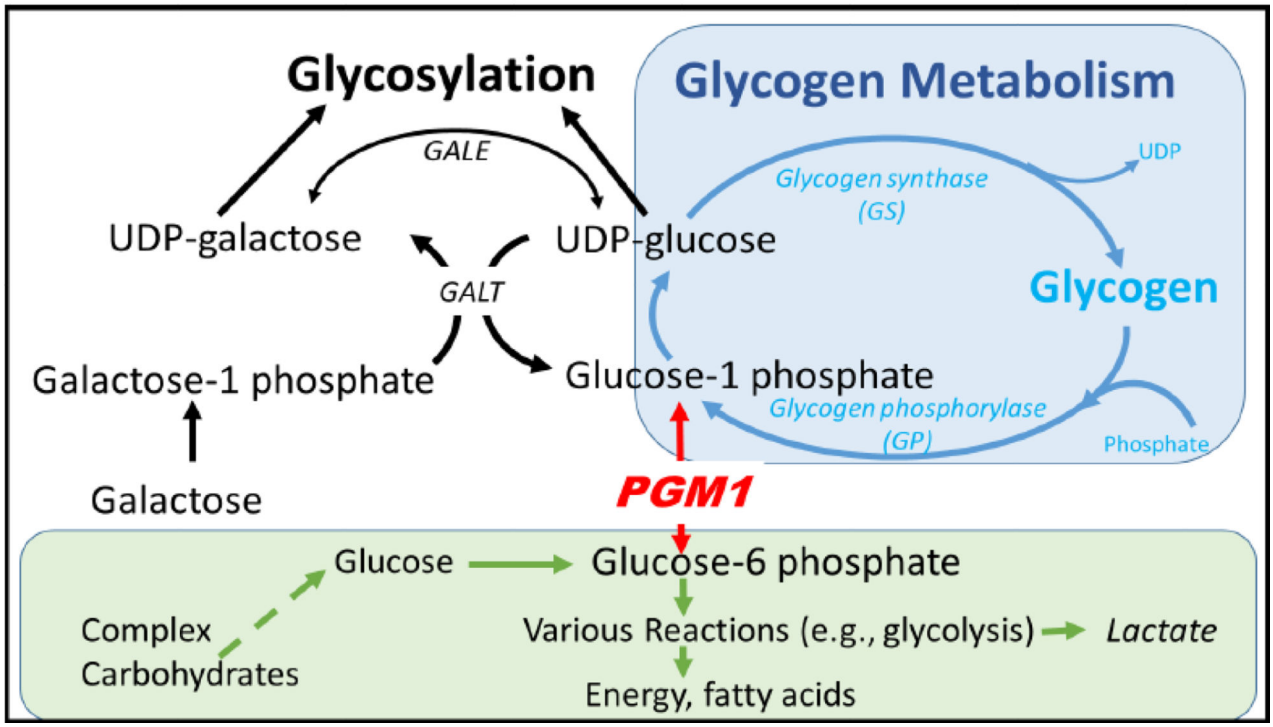

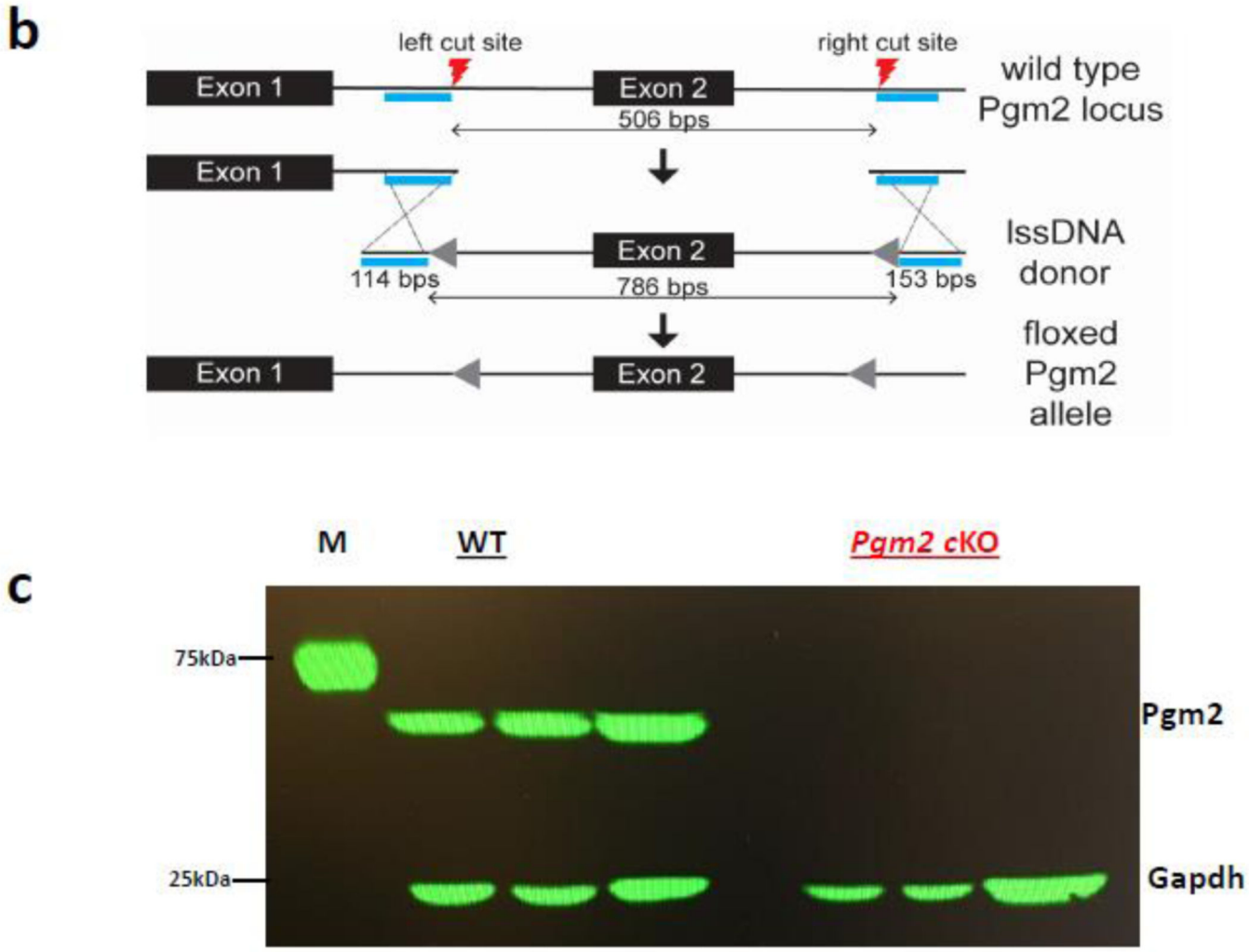

Fig. 1. Construction of *Pgm2 cKO* mice.

(a) PGM1 catalyzes the interconversion of glucose-1 phosphate and glucose-6 phosphate) and therefore, it plays a regulatory role in glycolysis, glycogenesis, glycogenolysis, and glycosylation.

(b) CRIPSR method of generating a floxed *Pgm2* allele (see text for details)

(c) Western Blot analysis of heart tissues from *Pgm2* cKO mice.

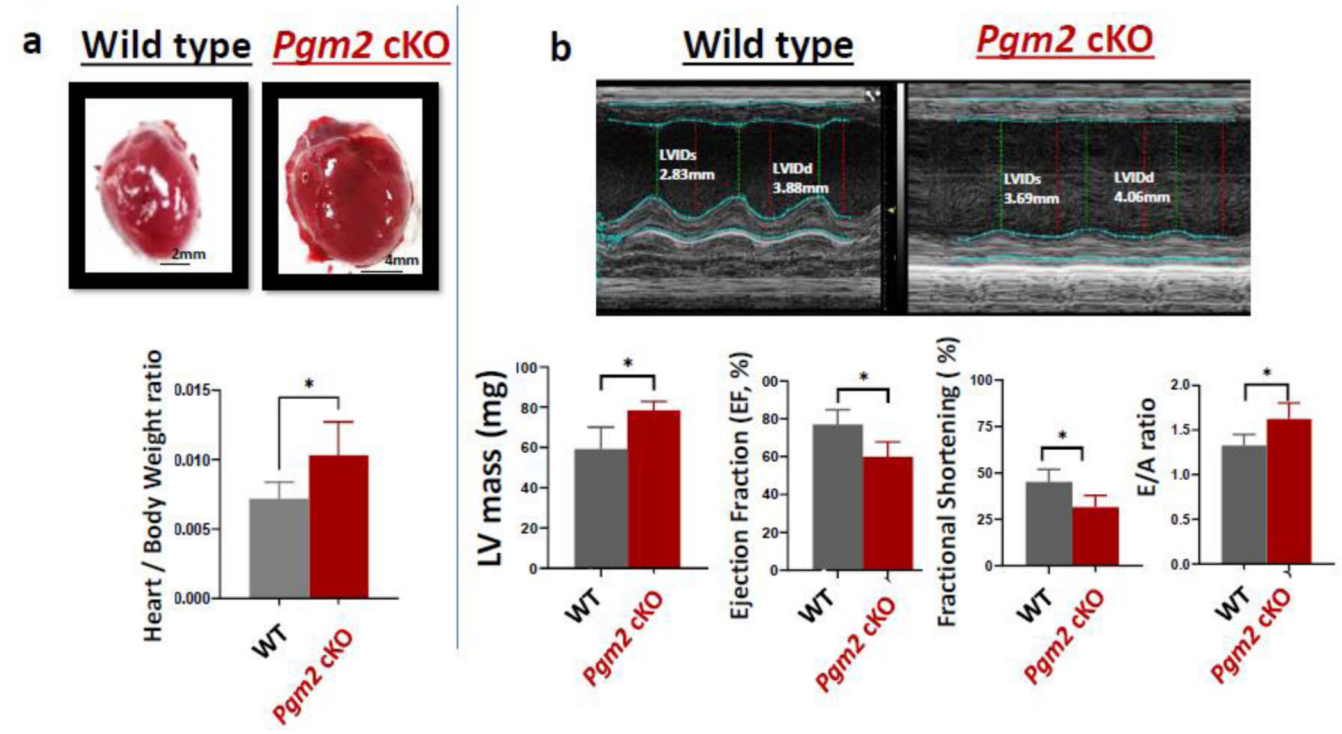

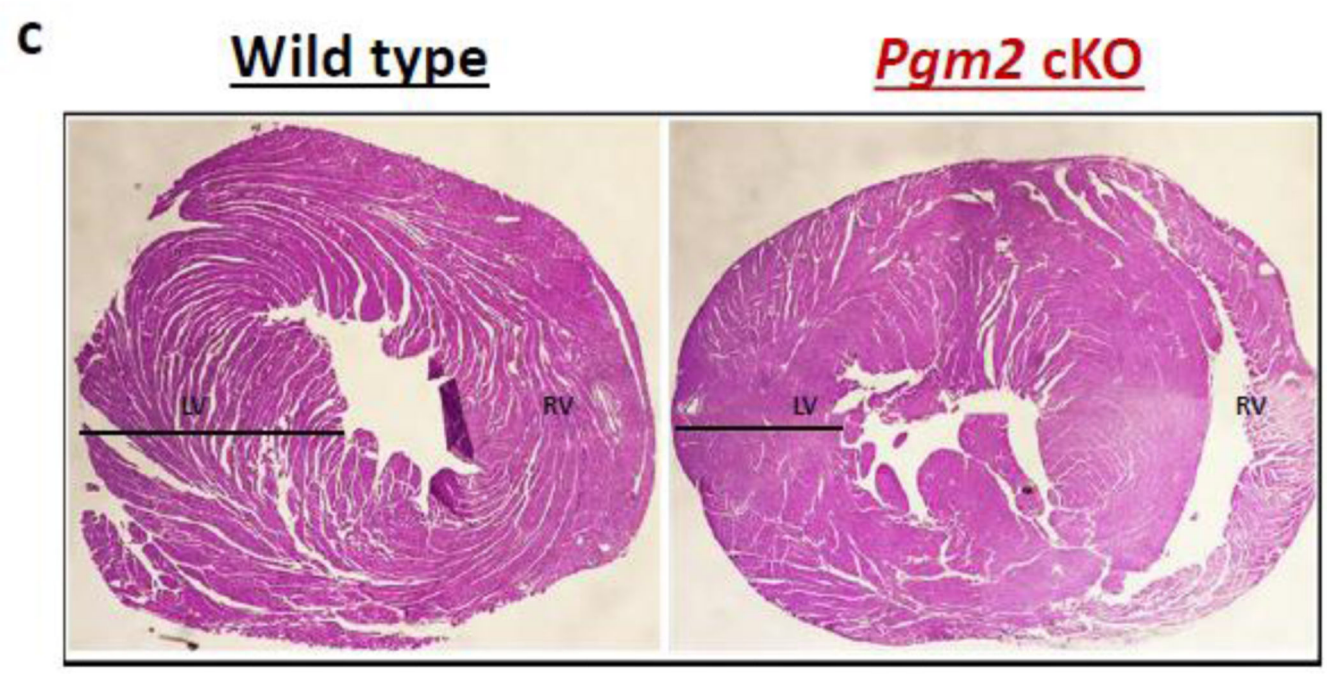

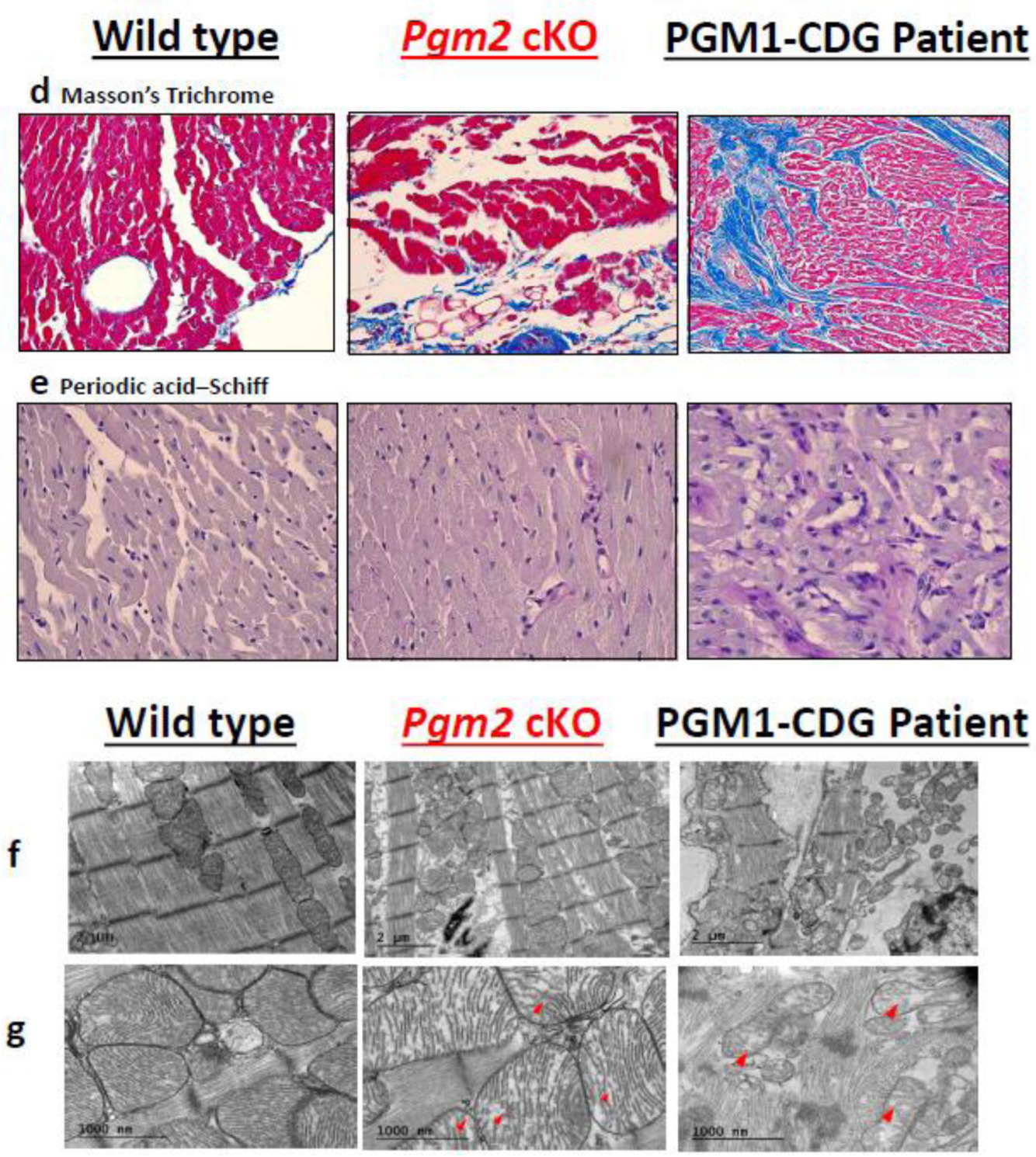

Fig. 2. Dilated heart and decreased cardiac functions in *Pgm2* cKO mice.

(a) Comparison of hearts from wild-type (WT) and *Pgm2* cKO mice 4 weeks after tamoxifen feeding N=6 for WT, N = 5 for *Pgm2* cKO.

(b) Echocardiography studies in WT and *Pgm2* cKO 12 weeks post-tamoxifen feeding. Data are mean±sem. N=3 for both WT and KO mice.
(c) Hematoxylin and Eosin (H & E) staining of WT and *Pgm2* cKO hearts.
(d) Masson's trichrome staining for fibrosis.
(e) PAS staining for glycogen.
(f) & (**g**) high magnification. Red arrows point to less organized mitochondrial cristae.

a

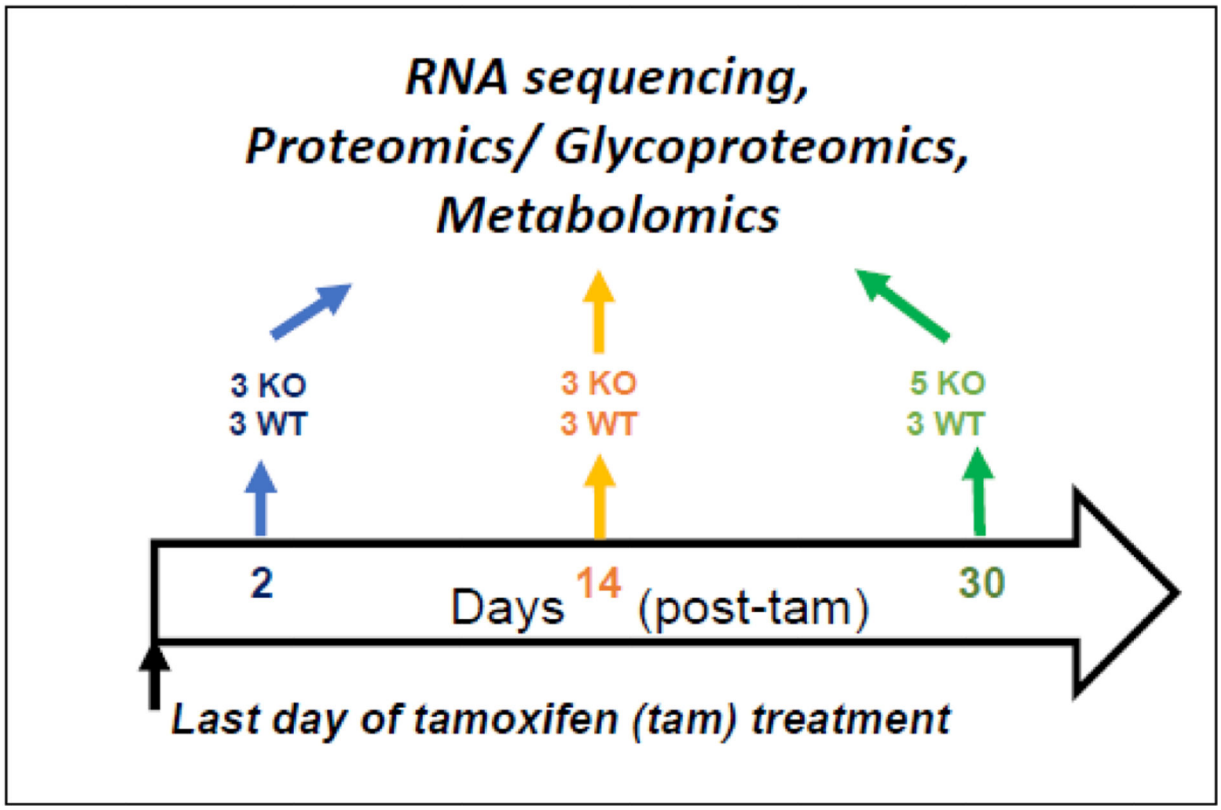

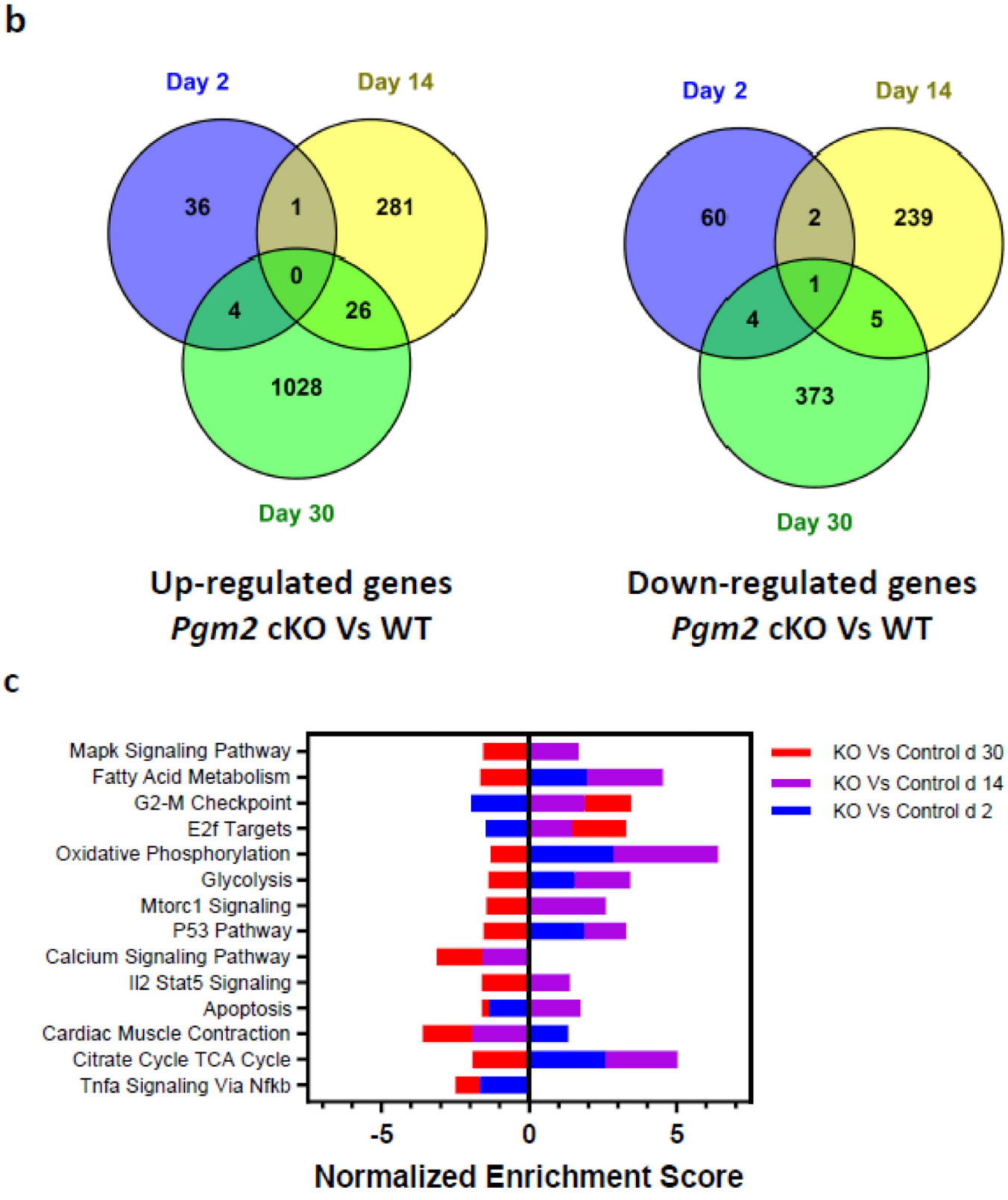

Fig. 3. Transcriptional dysregulation in *Pgm2* cKO mice.

(a) Experimental details.

(b) Differential gene expression at distinct stages of disease in KO vs. WT.

(c) Top 14 enriched pathways at different stages of disease in KO vs. WT.

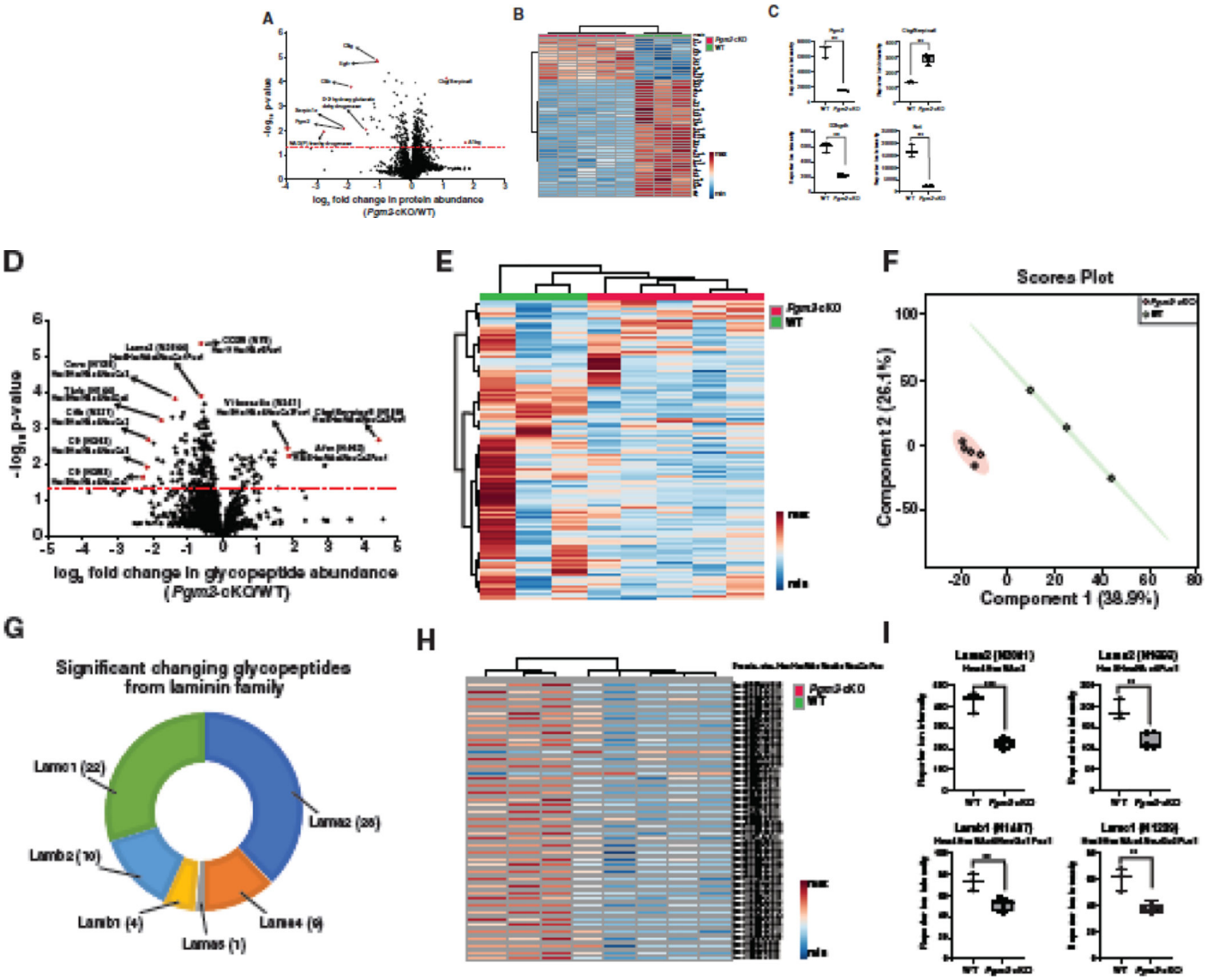

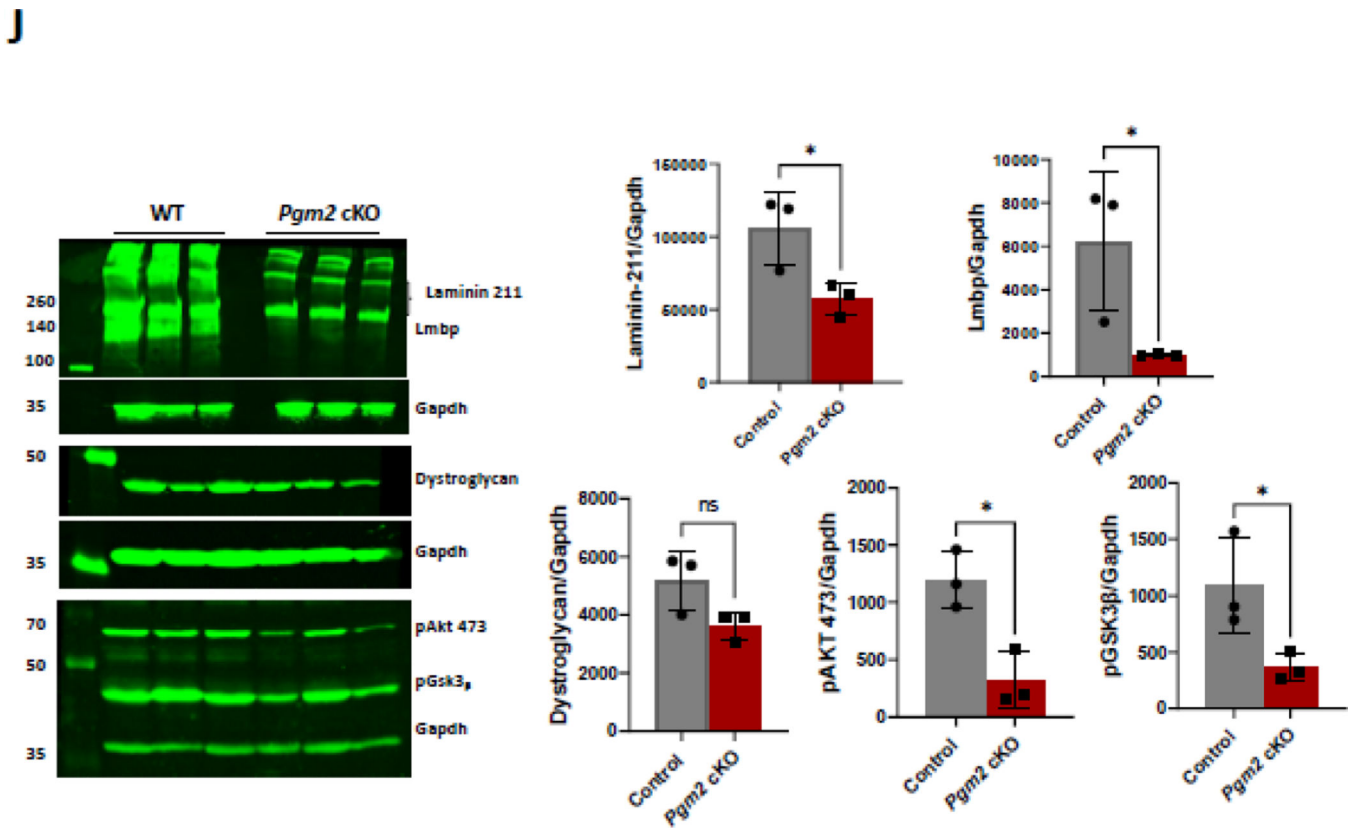

Fig. 4. Proteomics and glycoproteomcis analyses of *Pgm2* cKO and WT mouse hearts.

(a) Volcano plot depicting the differentially expressed proteins in *Pgm2* cKO at day 30 after induction. X-axis is $\log_2$ fold change (*Pgm2* cKO /WT) and Y-axis is the negative logarithm of p-value of student t test for significance. The horizontal dashed red line marks the cutoff for significance (<0.05). Some of the highly changing proteins are marked in red circles and protein names are provided.

(b) Heatmap of top 50 significantly changing proteins (p-value < 0.05) in *Pgm2* cKO mouse hearts. The pattern is color coded and gene names are given.

(c) Box plots showing reporter ion intensities of Pgm2, corticosteroid-binding globulin (Cbg/Serpina6), D-2-hydroxyglutarate dehydrogenase (D2hgdh) and NAD(P) transhydrogenase (Nnt) in WT and *Pgm2*-cKO mouse hearts. Y-axis is the reporter ion intensity of TMT channels. Each dot in the plots represent the individual sample. Data are expressed as mean ± SD. $p < 0.05$(*), $p < 0.01$(**), and $p < 0.001$(***).

(d) Volcano plot depicting the differentially expressed glycopeptides in *Pgm2* cKO at day 30 after induction. X-axis is $\log_2$ fold change (*Pgm2* cKO /WT) and Y-axis is the negative logarithm of p-value of student t test for significance. The horizontal dashed red line marks the cutoff for significance (<0.05). Some of the changing glycopeptides are marked in red circles and glycoproteins' names and glycosylation sites are drawn.

(e) Heatmap of all detected glycopeptides (p-value < 0.05) in *Pgm2* cKO and WT mouse hearts. The pattern is color coded.

(f) Partial Least Squares Discriminant Analysis (PLS-DA) based on reporter ion intensities for all identified glycopeptides of *Pgm2* cKO and WT. The percentage of total variance associated with each component is shown in brackets with the axis label.
(g) Number of glycopeptides correspond to different subunits of laminin family with significant aberrant glycosylation (p-value < 0.05) in *Pgm2* cKO mouse hearts.
(h) Heatmap of all significantly dysregulated glycopeptides corresponding to different laminin subunits illustrating their downregulation in *Pgm2* cKO. The subunit name, glycosylation site and glycan compositions on each glycosylation site are also shown on the right. The pattern is color coded.
(i) Box plots showing dysregulation in four representative glycopeptides of different laminin subunits. Y-axis is the reporter ion intensity of TMT channels. The subunit name, glycosylation site and glycan compositions on each glycosylation site are also shown on the top of box plots. Each dot in the plots represent the individual sample. Data are expressed as mean ± SD. $p < 0.05$(*), $p < 0.01$(**), and $p < 0.001$(***). Hex=Hexose; HexNAc=N-acetylhexosamine; NeuGc= N-glycolylneuraminic acid; Fuc=Fucose.
(J) Mis-glycosylated alpha 2 subunit (Lama2) of Laminin-211 interferes with the activation of the Pi3K/Akt signaling pathway in *Pgm2* cKO. Protein abundance was compared with WT control mice and normalized to Gapdh protein (n=3) $p < 0.05$(*)

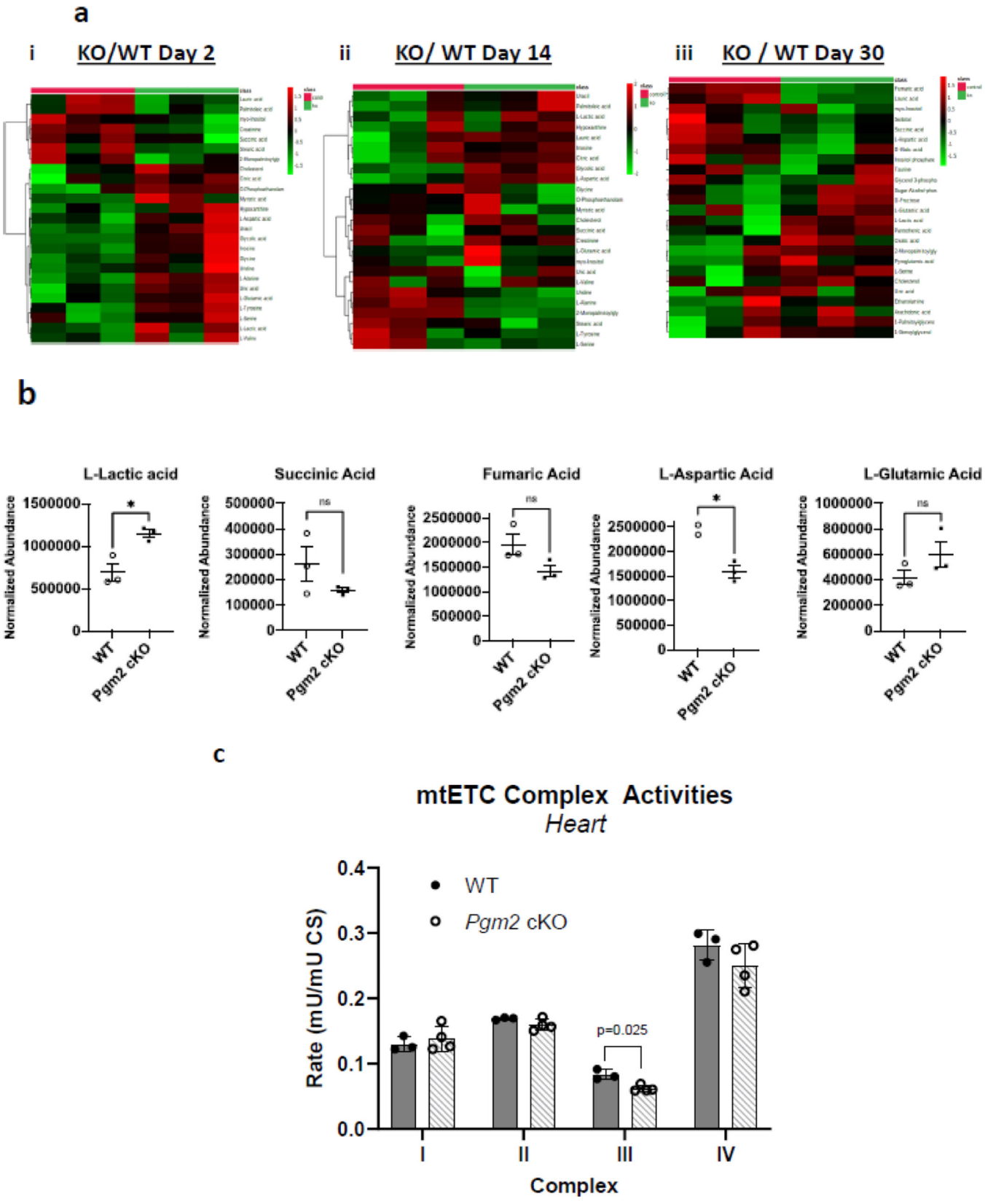

Fig. 5. Steady state metabolic profiling of WT and *Pgm2* cKO mouse hearts.

(a) Heat maps of differential metabolites at different stages of disease in KO vs. Control. The color represents the metabolite concentration of each sample calculated by peak area normalization method.

(b) Abundance of key TCA cycle metabolites in *Pgm2* cKO mice in 30 days after induction.

(c) Mitochondrial electron transport chain (mtETC) complex activities in murine heart homogenates from Pgm2 conditional knockdown (cKO) wildtype (WT) littermates. Pgm2 cKO hearts displayed a 25.5±5.6% reduction (Bonferroni-corrected p=0.025) in Complex III activity relative to WT littermates.

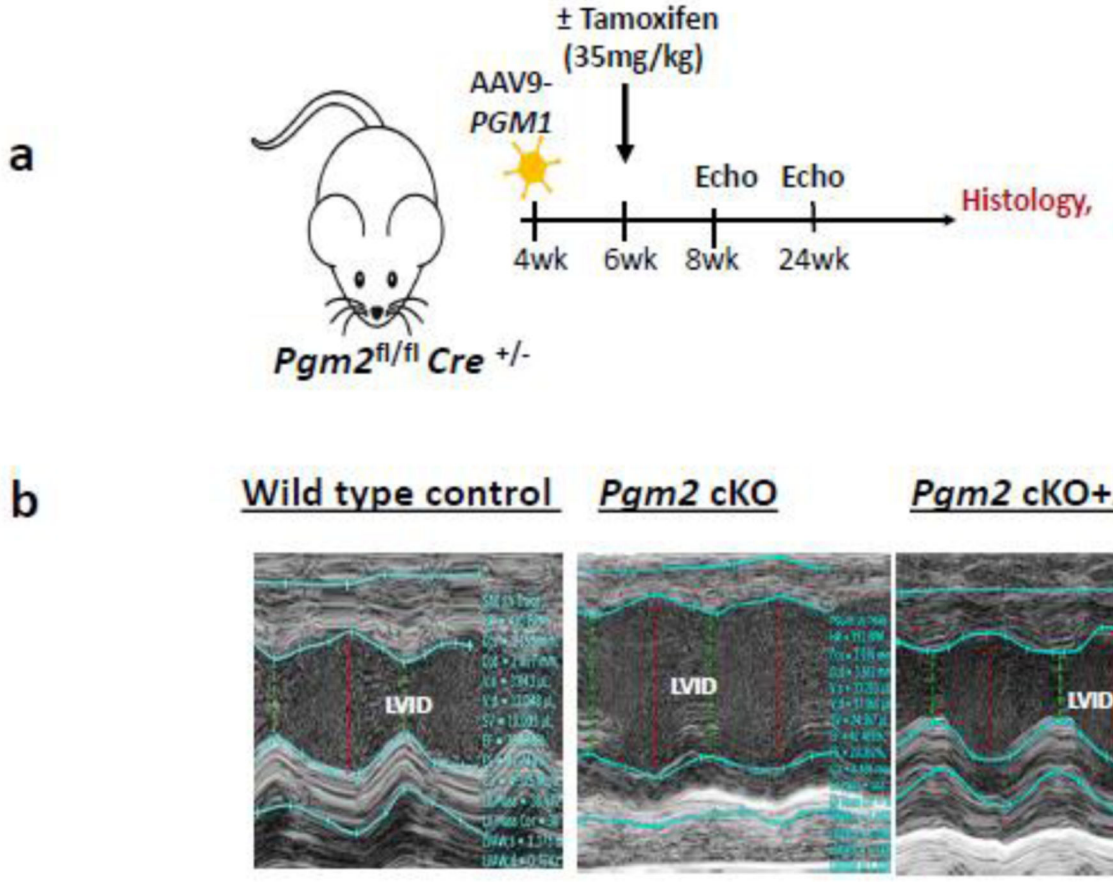

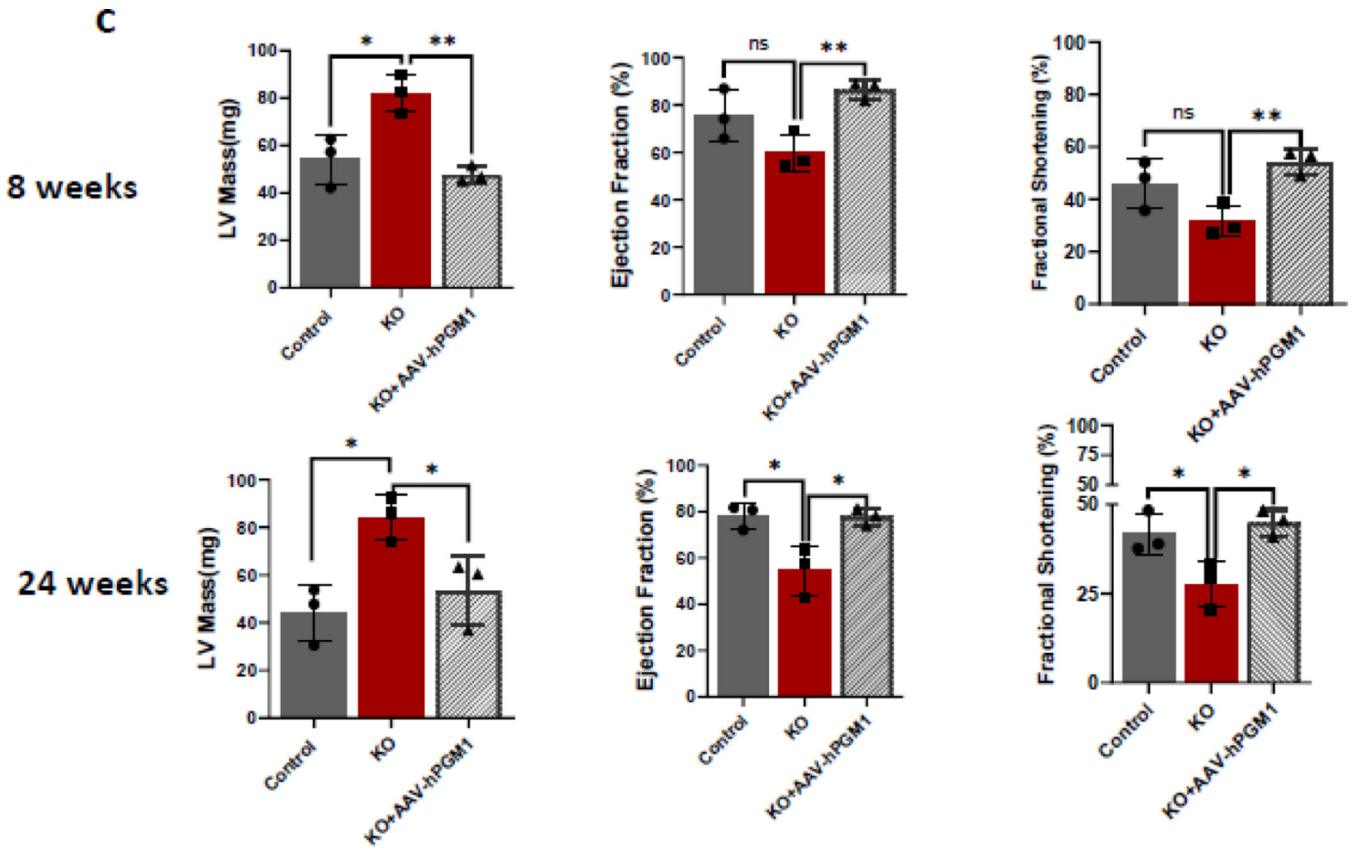

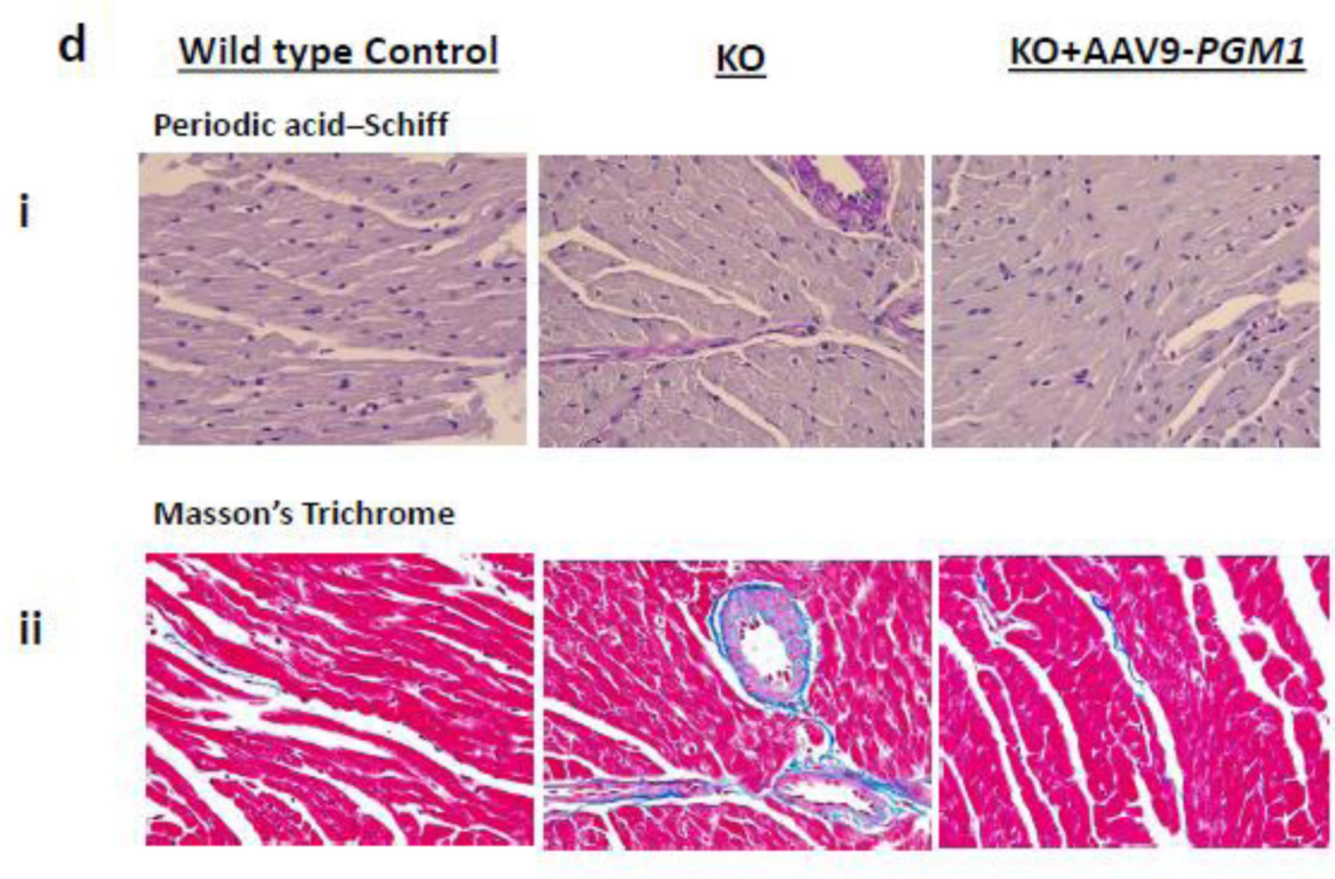

Fig. 6. AAV9-*PGM1* gene replacement prevents manifestation of cardiac functions in the *Pgm2* cKO mice

(a) Schematic of the overall experimental design. Cohorts (N= 3) of 4-week-old male *Pgm2*$^{fl/fl}$ mice were injected with 2.5E+13vg/kg of AAV9-*PGM1* and were subsequently subjected to tamoxifen feeding two weeks later. Echocardiography was performed at regular time intervals after tamoxifen feeding and the data were compared to untreated *Pgm2* cKO and wild type animals. **(b)** Representative echocardiographs of wild-type, *Pgm2* cKO and *Pgm2* cKO mice treated with AAV9-*PGM1* at 24 weeks of age.

(c) Quantified results of LV mass, Ejection fraction, Fractional Shortening obtained from echocardiography at 8 and 24 weeks of age, respectively.

(d) Histochemical studies of the heart tissues harvested from mice euthanized at 24 weeks.

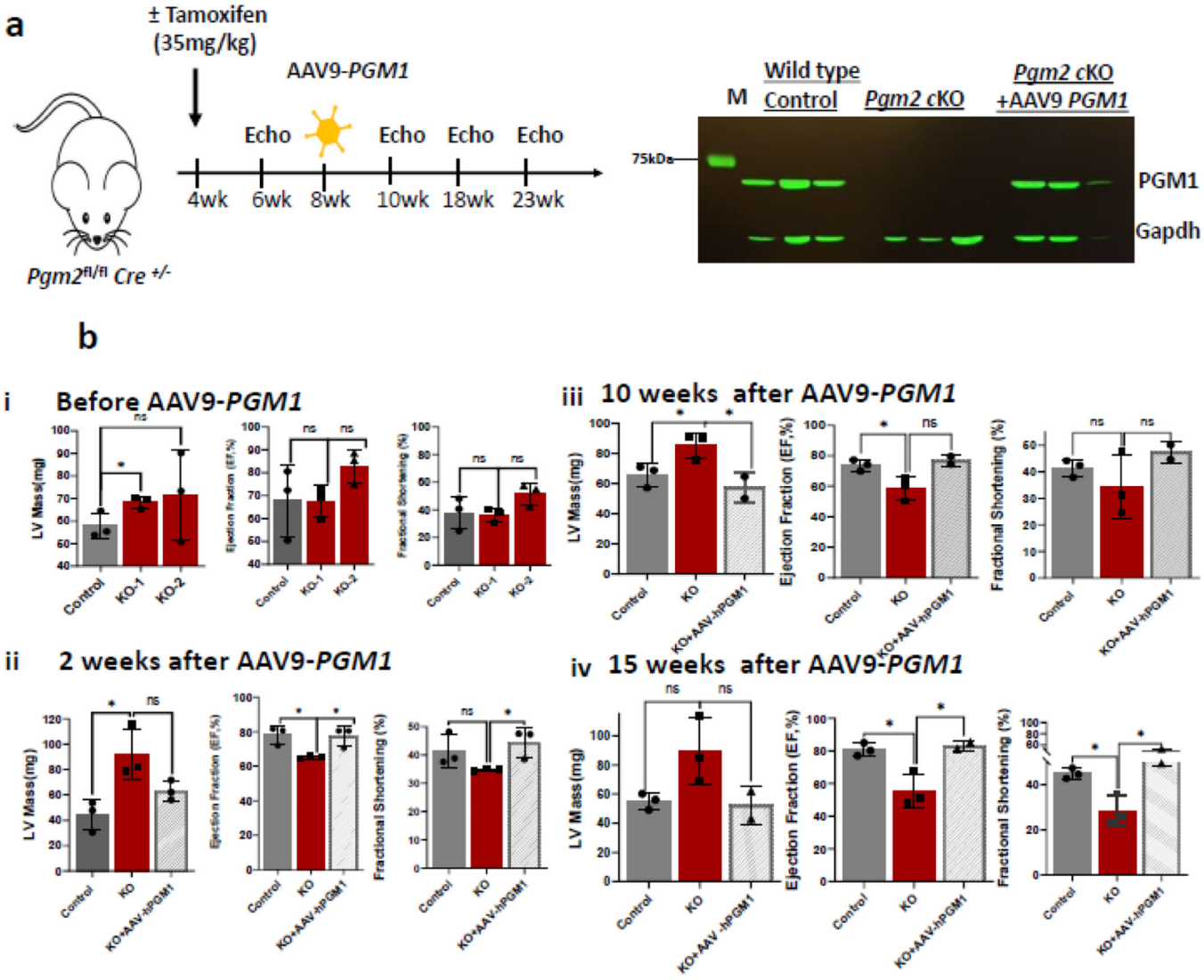

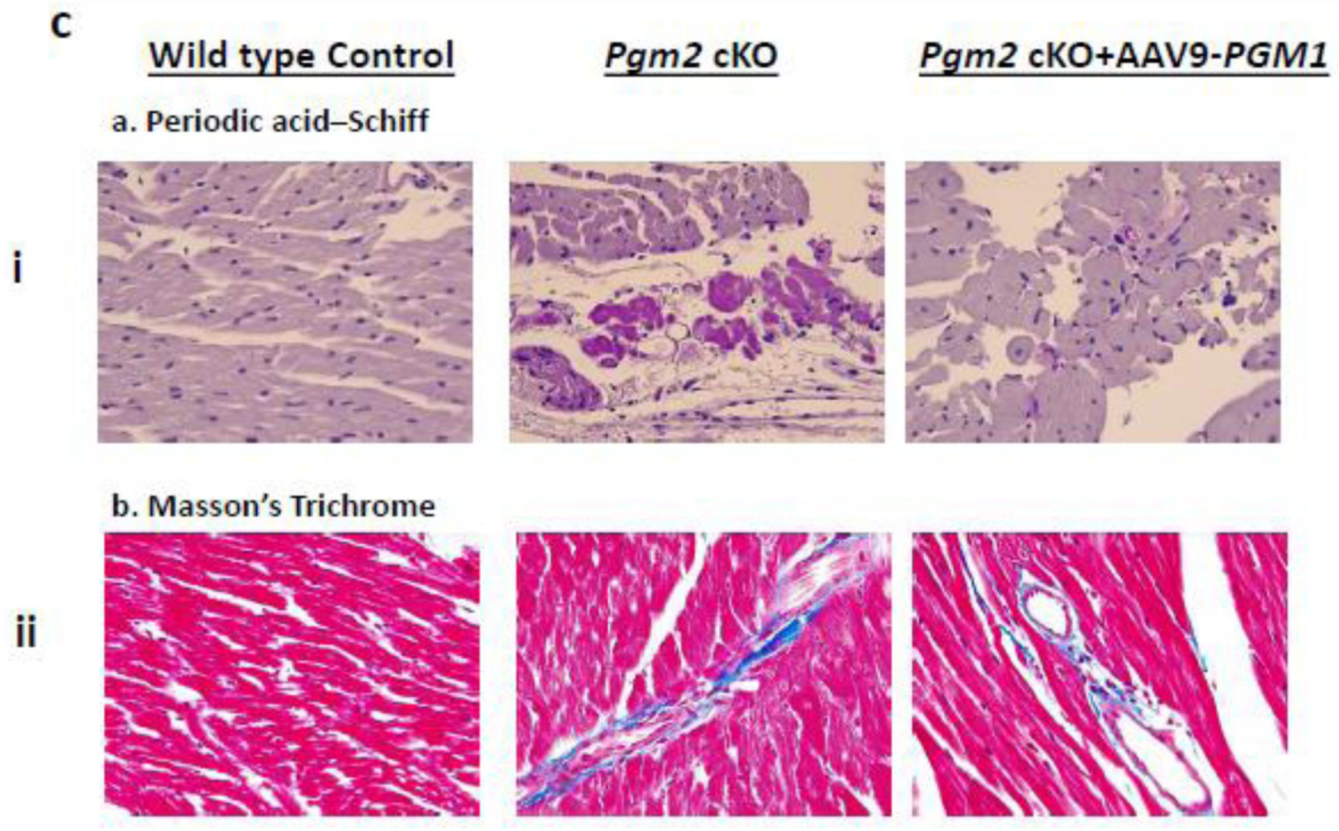

Fig. 7. AAV9-*PGM1* gene replacement halts/reverses the progression of cardiac functions in the *Pgm2* cKO mice

(a) Left: Schematic of the overall experimental design. Cohorts (n= 3/4) of 4-week-old male $Pgm2^{fl/fl}$ $Cre^{+/-}$ mice were fed with tamoxifen (35mg/kg body weight for 5 days). Echocardiography was performed two weeks later. Half of the cohorts were injected with 2.5E+13vg/kg of AAV9-*PGM1* two weeks later. Echocardiography was performed at regular time intervals and the data were compared to untreated *Pgm2* cKO and wild-type animals. Right: Western Blot to show reconstitution of PGM1 protein in the hearts of the treated animals.

(b) Quantified results of LV mass, Ejection fraction, Fractional Shortening obtained from different cohorts upon echocardiography at different time points after AAV9-*PGM1* treatment.

(c) Histochemical studies of the heart tissues harvested from mice euthanized at 17 weeks after AAV9-*PGM1* therapy.

Table 1

Echocardiogram findings in an individual affected with PGM1-CDG and *Pgm2* cKO mice

Human data are from a single individual with PGM1-CDG associated DCM whereas mouse data are the average of 3 mice.

Human Patient	**Age**		
	3 months	**6 months**	**10 months**
LVIDs (MM)	1.6 cm	2.3 cm	2.9 cm
LVIDd (MM)	2.8 cm	3.1 cm	3.1 cm
LVPWd (MM)	0.87 cm	0.45 cm	0.43 cm
EF (%)	72	54	10

***Pgm2* cKO mice**	**Age**			
	1.5 months	**2.5 months**	**4.5 months**	**5.75 months**
LVIDs (MM)	1.5mm	2.2mm	1.84mm	2.8mm
LVIDd (MM)	2.6mm	3mm	2.7mm	4.2mm
LVPWd (MM)	0.98mm	1.1mm	0.92mm	0.86mm
EF (%)	72	65	61	59

Abbreviations: LVIDs and LVIDd, left ventricular internal diameter at end-systole; LVPWd, Left ventricular posterior wall thickness at end diastole and end systole; EF, ejection fraction

Table 2

Demographic, genetic and cardiac features of 6 PGM1-CDG patients enrolled in Natural History study.

Patients	Age #/Sex	*PGM1* variants	DCM	Current LVEF %	Tricuspid valve insufficiency	Negative T waves	ST elevation	Arrhythmia	Tachycardia	Cardiac improvement on D-gal *
P1[7]	27/F	c.988G>C, c.1129G>A	Yes	38–45	+	+	+	-	-	No
P2[43]	30/F	c.313A>T, c.200T>G	No	64	+	+	-	-	+	No
P3[43]	2/F	c.787G>T, c.988G>C	Yes	55	+	+	-	-	+	No
P4[43]	5/M	c.265G>A, c.988G>C	No	57–76.9	+	+	-	-	-	No
P5	2/M	c.1544G>A, c.1544G>A	Yes	35%	+	-	-	-	-	No
P6	2/F	c.1544G>A, c.1544G>A	Yes	10%**	+	-	-	+	+	No

age at the time of the publication

* improvement of cardiac related issues on galactose therapy; abbreviations: NR- not reported. First reported in Tegtmeyer et al 2014[7]; First reported in Perales-Clemente et al 2021[42]. Abbreviations: DCM- dilated cardiomyopathy, F-female, M-male, P- patient